

**INTERSTITIAL CELLS OF CAJAL IN NORMAL HUMAN ALIMENTARY TRACT: AN IMMUNOHISTOCHEMICAL STUDY**

Mohamed Abdel Hafez; Amal Mostafa Abbas; Dina Mohamed Radwan and Zeinab El Meadawy

Histology Department, Faculty of Medicine, Cairo University

**Abstract**

**Background/Objective:** Interstitial cells of Cajal (ICC) are c-kit positive immunoreactive cells which are thought to play an important role in the control of gut motility. The work aimed at studying the morphology of ICC and precisely localize their regional and transmural pattern of distribution in normal human alimentary tract.

**Material and Methods:** The study included 102 normal human alimentary tract specimens obtained from male patients with a mean age  $37.92 \pm 8.53$ . All sections were stained with hematoxylin and eosin and c-kit immunohistochemical staining. Immunohistochemically stained sections were submitted for a computer aided image analytical study to detect the area percent of immunoreactive cells. The data obtained was statistically analyzed.

**Results:** ICC could not be demonstrated in H&E stained sections. Immunohistochemically, two morphological subtypes of ICC were recognized, a spindle bipolar and stellate multipolar forms. ICC were detected in the myenteric plexus layer of the esophagus, corpus, pylorus, small intestine, colon and rectum. Intramuscular ICC could be demonstrated in the esophagus, fundus, corpus, pylorus, colon, rectum and anal canal. ICC at the deep muscular plexus were found only in the small intestine. In the pylorus, colon and rectum, ICC were also found at the submucosal border of the circular muscle layer.

**Conclusion:** The wide distribution of ICC all over the human alimentary tract is compatible with their physiological role being important mediators of gut motility.

**Key Words:** interstitial cells of Cajal ; ICC ; alimentary tract ; immunohistochemistry; c-kit

**INTRODUCTION**

Interstitial cells of Cajal (ICC) are groups of cells found throughout the gut from the esophagus to the anus. ICC are thought to play an important role in the control of gut motor activity; acting as pacemakers (Thuneberg, 1982), intermediaries in the neural control of gut muscular activity (Daniel and Posey-Daniel, 1984), and spatial coordinators of gut motility (Farraway *et al.*, 1995). The particular function that ICC can perform may be dependent on their location within the gastrointestinal tract (Ward *et al.*, 2002). Abnormal distribution of ICC has been reported in several human diseases and abnormal functions of ICC might actually be involved in many disorders of the gastrointestinal tract (Wedel *et al.*, 2002). Among the gut motility disorders having direct relation to ICC are the infantile hypertrophic pyloric stenosis (Langer *et al.*, 1995), Hirschsprung's disease (Vandewinden *et al.*, 1996), gastrointestinal

stromal tumors (Kindblom *et al.*, 1998), diabetic gastrointestinal dysfunction (Zhang *et al.*, 2002) and chronic idiopathic intestinal pseudo-obstruction (Jain *et al.*, 2003). ICC could not be identified in routine hematoxylin and eosin stained sections (Hagger *et al.*, 1998). They were hardly recognized by the electron microscope (Faussone-Pellegrini *et al.*, 1990) and immunoelectron microscopy (Wang *et al.*, 2000). The discovery of the selective expression of the kit receptor in ICC within the alimentary tract and its crucial role in the normal development of ICC and their pacemaker activity has produced a powerful new tool in the investigation of these cells and their function in normal and pathological conditions (Maeda *et al.*, 1992). The expression of c-kit has been evaluated by mRNA detection, flowcytometry as well as immunohistochemistry (Arber *et al.*, 1998). The distribution of ICC in normal human adults was difficult to define because there

were conflicting data on their distribuion in the normal human alimentary tract (**Rumessen and Thuneberg, 1996**). Furthermore, the density of ICC might vary within regions of the alimentary tract making comparisons between diseased groups and controls prone to errors (**Poole et al., 2003**). Hence, this work was planned to study the morphology of ICC and to evaluate the transmural and regional pattern of their distribution in the normal human alimentary tract. This could facilitate the rapid progress towards identifying their exact role in physiological and pathological conditions.

## MATERIAL AND METHODS

### Materials:

The present study was carried out on 102 normal human surgical specimens from different segments of the alimentary tract. Most of the specimens were obtained from normal safety margins of male patients undergoing surgery for cancer. These specimens were received from the Pathology Departments of both, Faculty of Medicine and National Cancer Institute (NCI), Cairo University during the period from November 2003 to December 2004. The patients' age ranged from 22 to 50 years (mean age;

37.92±8.53). Relevent data on the patients and the indications for surgery are given in Table (1).

The specimens were fixed in 10 % formol saline and paraffin blocks were performed. Sections of 5 µm thickness were stained with hematoxylin and eosin and carefully examined microscopically to exclude infiltration by malignant or inflammatory cells. Tissue was defined as normal when the selected area was not invaded by the tumor. Immunohistochemical staining for the c-kit (**Bancroft and Cook, 1994**) was performed using the primary antibody c-kit (CD117) was a polyclonal rabbit, antihuman, supplied by DAKO corporation Lab. (USA) and was used at a dilution of 1:200 with DAKO antibody diluent having background reducing components. The detection system "DAKO LSAB2 System Peroxidase was used applying DAB chromogen to demonstrate antigen in the cells. Counterstaining of the sections was done with Mayer's hematoxylin reagent. Normal human breast tissue was used as a positive control, whereas as a negative control, an additional slide of the alimentary tract was treated with antibody diluent instead of the primary antibody. Cells positive for c-kit showed brown cytoplasmic deposits.

*Table 1. Topographic distribution, age range and surgical indication of studied 102 normal alimentary tract specimens.*

<b>Topology</b>	<b>No.</b>	<b>Age range (years)</b>	<b>Surgical indication</b>
<i>Esophagus</i>	7	23-40	Cancer larynx
<i>Fundus</i>	5	25-50	Cancer stomach
<i>Corpus</i>	5	25-50	Cancer stomach
<i>Antrum</i>	8	30-50	Cancer stomach
<i>Duodenum</i>	8	30-50	Cancer head of pancreas
<i>Jejunum</i>	6	32-48	Bypass for obesity
<i>Ileum</i>	9	28-47	Cancer colon
<i>Cecum&amp;appendix</i>	9	35-50	Cancer colon
<i>Ascending colon</i>	9	35-50	Cancer colon
<i>Transverse colon</i>	10	34-48	Cancer colon
<i>Descending colon</i>	11	22-49	Cancer colon
<i>Rectum</i>	10	25-50	Cancer rectum
<i>Anal canal</i>	5	39-50	Cancer rectum

### Morphometric Study

The c-kit immunoreactivity in the form of dense brown deposits were submitted for image analysis using Leica Imaging System, Ltd., Cambridge, England (Leica Qwin). The image analyzer was first calibrated to convert the measurement unit produced by the image analyzer program (pixels) into actual micrometer units. Ten fields from each section were selected and the area percent of the dense brown deposits were measured by the image analyzer in relation to a standard measuring frame which was 7286.8  $\mu\text{m}^2$  using magnification X400. Measurements were done for each alimentary tract segment in the different layers of its wall. The area percent obtained from the image analyzer was subjected to statistical analysis.

### Statistical Analysis

The statistical analysis was performed using the arithmetic mean (X), standard deviation (S.D.) and student "t" test according to **Mould (1989)**. All statistical analyses were done on an IBM PC using the statistical software "Statistica for Windows" Version 5. Results were considered significant when probability (p) was  $\leq 0.05$ .

## RESULTS

### Histological Results

Examination of H&E-stained sections of the esophagus revealed a mucosa formed of non-keratinized stratified squamous epithelium resting on a connective tissue corium (Fig 1, A). Submucosal plexus consisting of ganglionic cells and nerve strands (Fig, 1,B), oesophageal mucus glands and small lymphoid follicles (Fig.1,C) were seen in the submucosa. In the upper third of esophagus, the muscularis externa was exclusively formed of striated muscle bundles separated by connective tissue septa containing nerve bundles and myenteric plexus (Fig. 1, D), In the middle third, muscularis externa consisted of smooth and striated muscle fibers (Fig 1,E), whereas only smooth muscle fibers could be seen in the lower third (Fig. 1,F). Sections in the human gastric fundus and corpus revealed that mucosa formed of long, closely-related glands separated by a lamina propria extending to the muscularis mucosa (Fig.2, A). Muscularis externa consisted of smooth

muscle arranged as inner oblique, middle circular and outer longitudinal layers. Myenteric plexus was noticed inbetween the circular and longitudinal muscle layers (Fig.2,B). Sections in the human pylorus revealed the widely separated pyloric glands with their deep pits (Fig.2,C). Muscularis externa consisted of thick inner circular and thin outer longitudinal muscle layers with myenteric plexus inbetween (Fig.2,D). Sections in the different levels of human small intestine were characterized by the appearance of intestinal villi and crypts of Lieberkuhn in the mucosa. In the duodenum, the villi were broad and long (leaf-like). Mucous secreting glands (Brunner's glands) were seen in the submucosa in most of the duodenal specimens (Fig.3,A). Jejunal villi were tongue-shaped (Fig. 3,B). In the ileum, the villi were slender (finger-like) (Fig.3,C). In all levels of the small intestine, submucosal plexus could be observed (Fig.3, D) and muscularis externa with its two layers could be seen with myenteric plexus inbetween (Fig.3,E). Sections of human cecum, appendix, ascending, transverse, descending colon and rectum showed crypts in the mucosa which were lined by tall columnar cells with basal oval nuclei and were rich in goblet cells (Fig. 4, A). Submucosal plexus could be seen in the upper part of the submucosa (Fig.4, B). Muscularis externa was formed of inner circular and outer longitudinal muscle layers with myenteric plexus inbetween (Fig.4,C). The mucosa of the appendix revealed large lymphoid follicles extending to the submucosa (Fig.5,A). Sections in the human rectum revealed the lamina propria rich in lymphoid follicles and diffuse lymphoid tissue (Fig5, B). Pacinian corpuscles and submucosal plexus could be observed in the submucosa of the rectum (Fig.5,C). At the recto-anal junction, the simple columnar epithelium of rectum, was replaced by non-keratinized stratified squamous epithelium (Fig.6,A). The inner circular muscle layer thickened to form the internal anal sphincter (Fig.6, B). At the terminal end of the anal canal, the anal orifice was covered by skin (Fig. 6,C). At the anal orifice, the external anal sphincter was formed of striated muscle fibers (Fig.6,D).

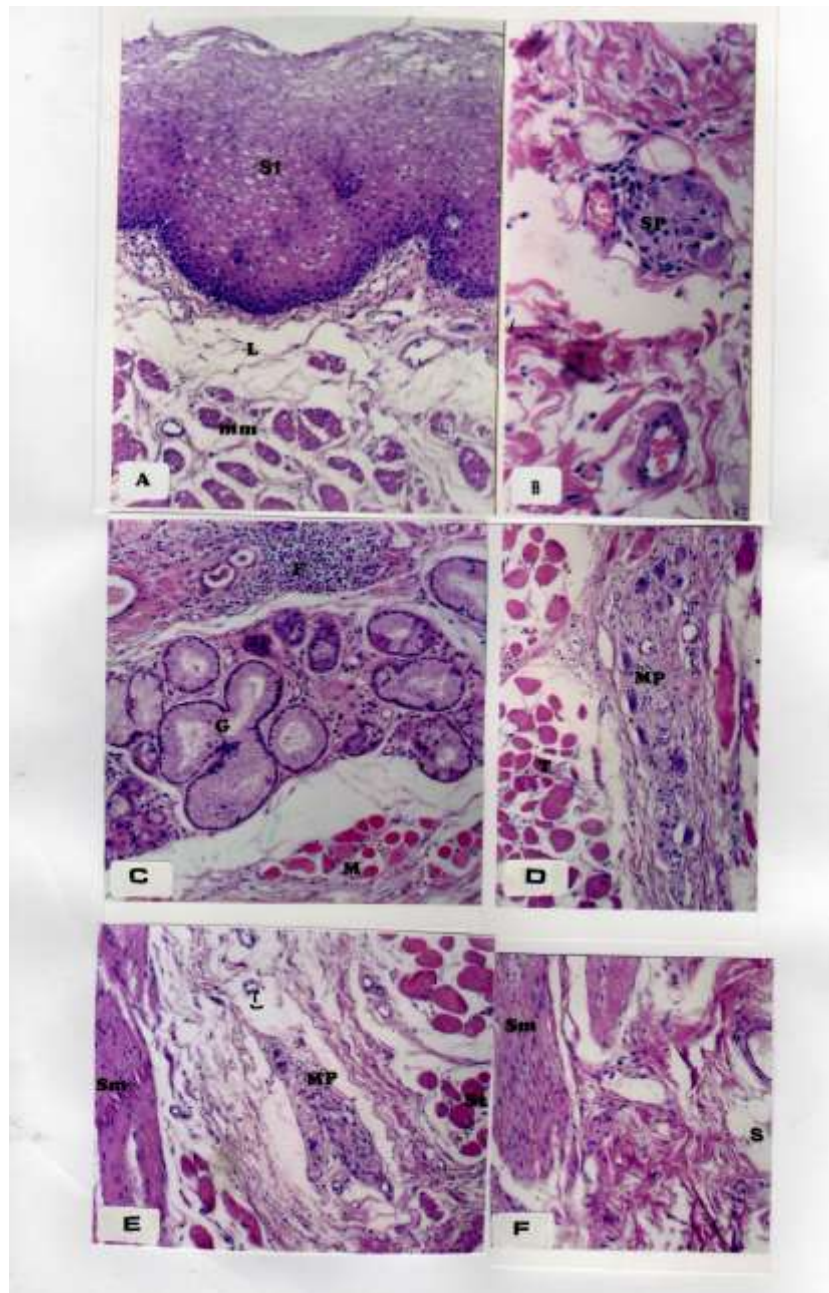


**Fig. (1):** Photomicrographs of sections in the human esophagus revealing: **{A}** mucosa is formed of non-keratinized stratified squamous epithelium (St), lamina propria (L) and muscularis mucosa (mm) (*H&E, X100*), **{B}** submucosa containing a submucosal plexus (SP) (*H&E, X200*), **{C}** submucosa containing mucous glands (G) a small lymphoid follicle (F) and apart of muscularis externa (*H&E, X100*), **{D}** myenteric plexus (MP) enclosed between the striated muscle fibers which were cut transversly (T) in the upper third (*H&E, X100*), **{E}** in the middle third, muscularis externa is formed of smooth (Sm) and striated (St) muscle fibers with a myenteric plexus (MP) inbetween (*H&E X100*), **{F}** muscularis externa with smooth muscle (Sm) bundles in the lower third. Part of the submucosal (S) is seen (*H &E X 100*).

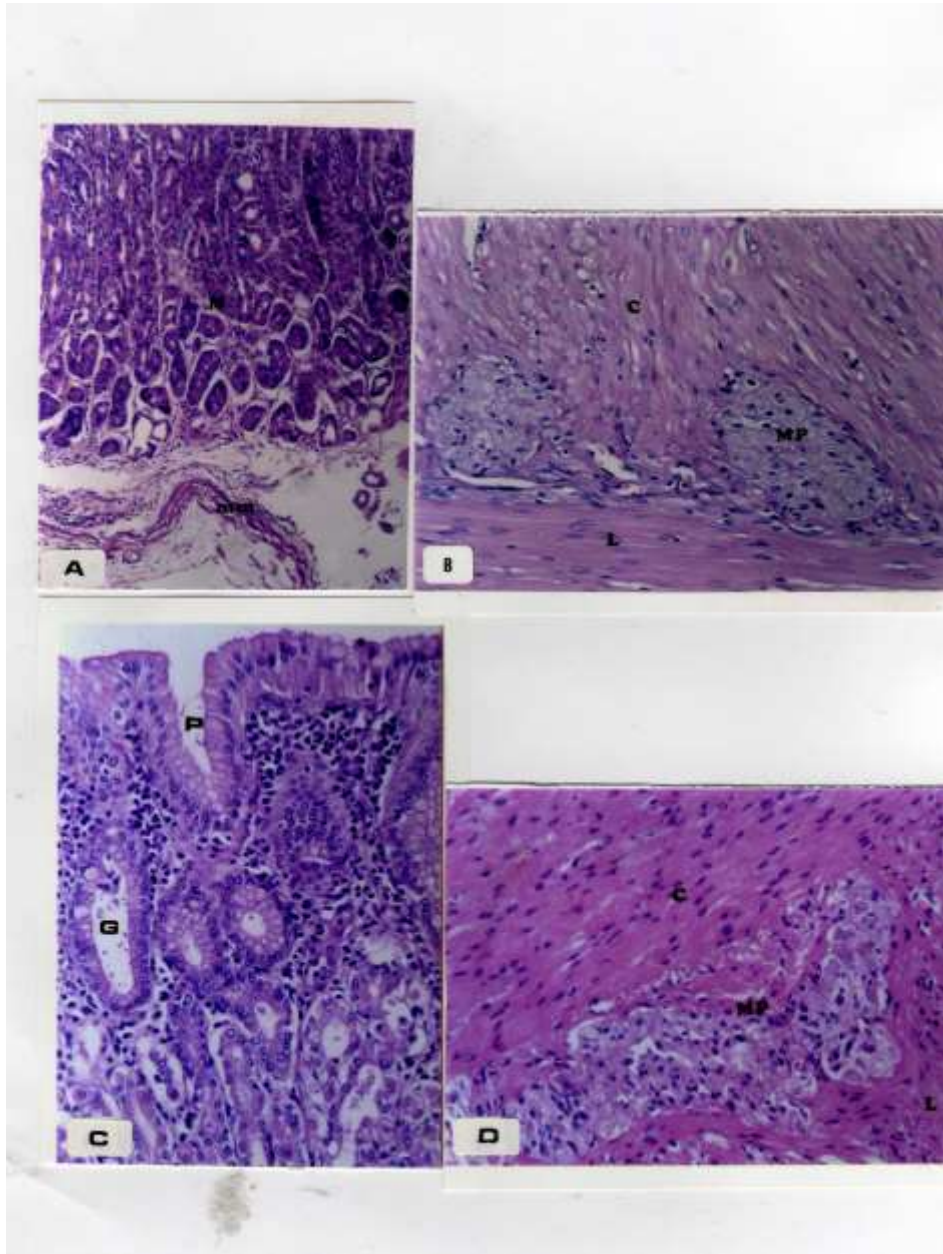


**Fig. (2):** Photomicrographs of sections in the human stomach revealing: **{A}** Fundic region with mucosa (M) being formed of long, closely-packed fundic glands, lamina propria and muscularis mucosa (mm) (*H&E, X100*), **{B}** the muscularis externa with a myenteric plexus (MP) enclosed between circular (C) and longitudinal (L) muscle layers (*H&E, X200*), **{C}** pyloric glands (G) opening on the surface by gastric pits (P). Their secretory parts are cut in cross and oblique sections (*H&E, X200*), **{D}** The muscularis externa with its two layers of smooth muscle; thick inner circular (C) and thin outer longitudinal (L) and a myenteric plexus (MP) in between (*H&E X 200*)

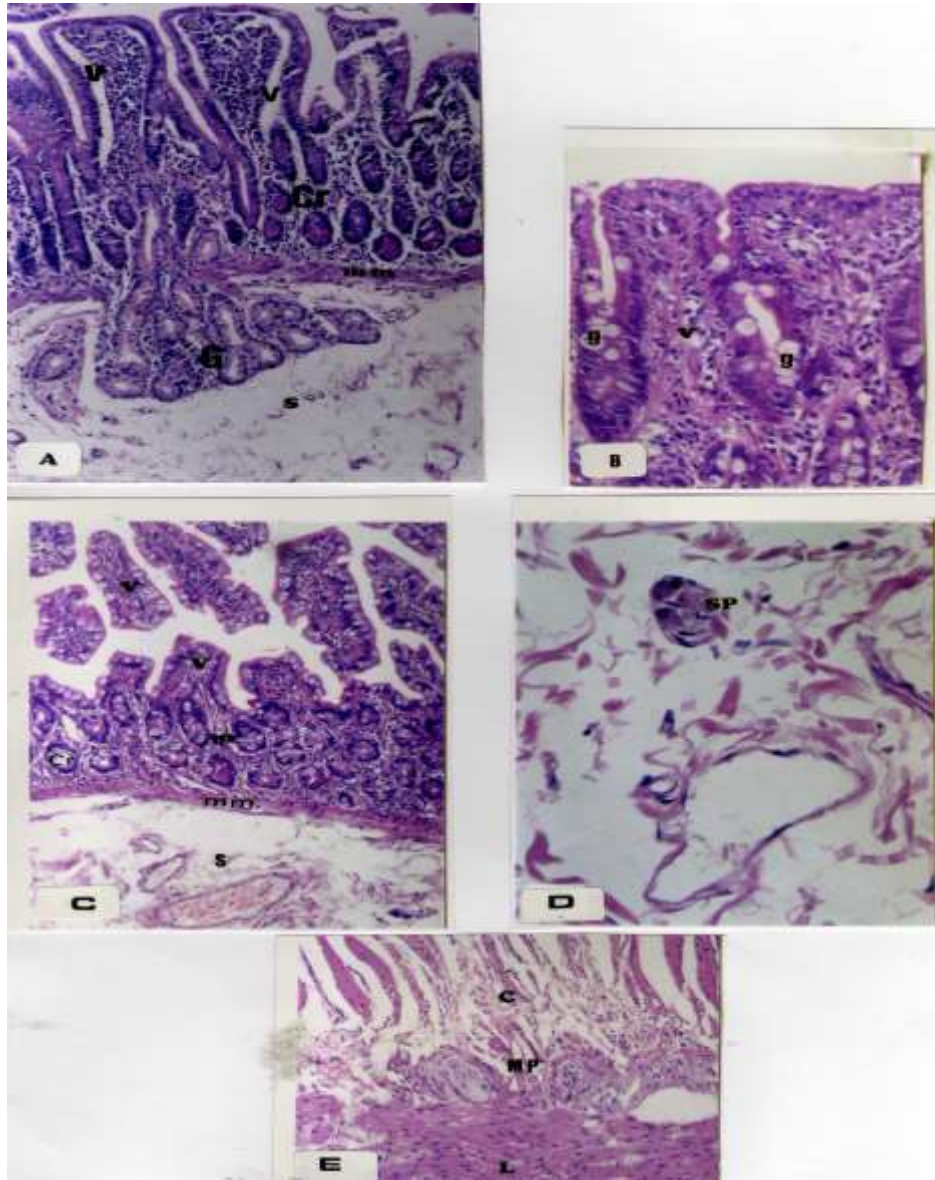


**Fig. (3):** Photomicrographs of sections in the human small intestine revealing: **{A}** the duodenal mucosa formed of broad and long (leaf-like) villi (V), crypts of Liberkuhn (Cr), lamina propria and muscularis mucosa (mm). Brunner's glands (G) are seen in the submucosa (s) opening by ducts into the bottom of the crypts (*H&E*, X100), **{B}** jejunal mucosa showing tongue-shaped villi (V) formed of a central core of connective tissue, covered by absorptive simple columnar cells and goblet cells (g) (*H&E*, X200), **{C}** ileal mucosa formed of slender (finger – like) villi (V), crypts (Cr), lamina propria and muscularis mucosa (mm). part of submucosa (s) is seen (*H&E*, X100), **{D}** a submucosal plexus (SP) (*H&E*, X400), **{E}** the muscularis externa formed of inner circular (C) and outer longitudinal (L) muscle layers. A myenteric plexus (MP) could be seen enclosed between the two muscle layers (*H&E*, X100).

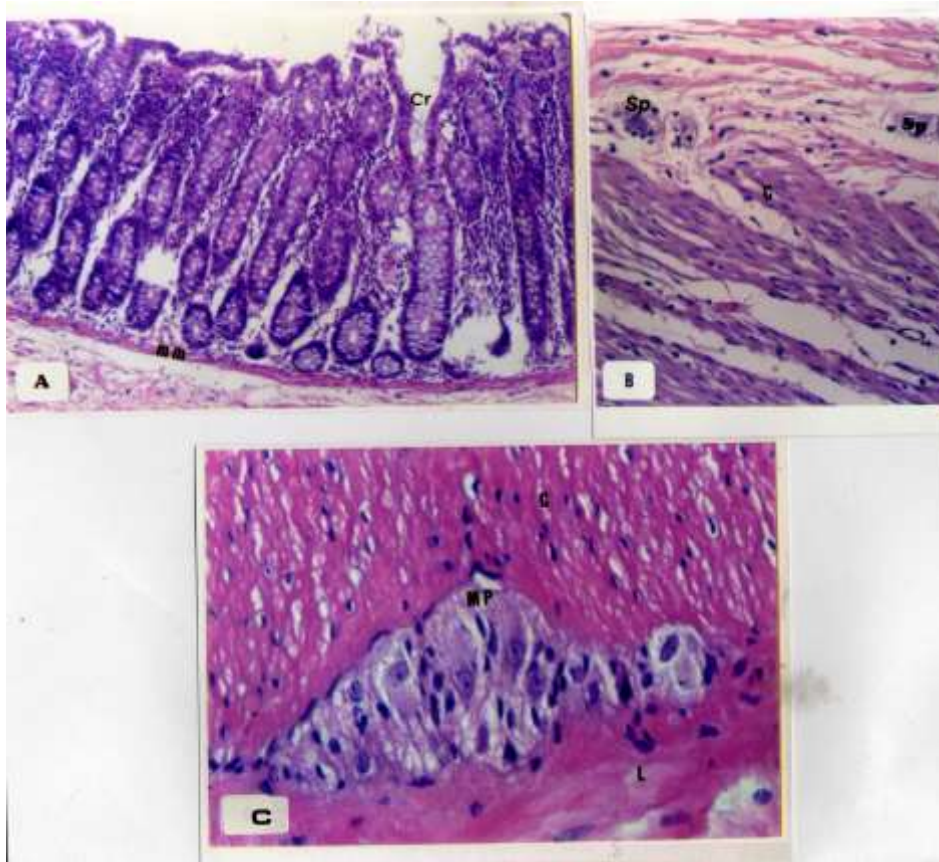


**Fig. (4):** Photomicrographs of sections in human large intestine showing: **{A}** colonic mucosa containing numerous crypts (Cr) with abundant goblet cells. Muscularis mucosa (mm) is also seen (*H&EX100*), **{B}** a submucosal plexus (sp) in the lower part of the submucosa close to the inner circular layer of the muscularis externa (C) (*H&E X 200*), **{C}** Muscularis externa with the inner circular (C) and the outer longitudinal (L) muscle layers and myenteric plexus (MP) in between (*H&EX400*).

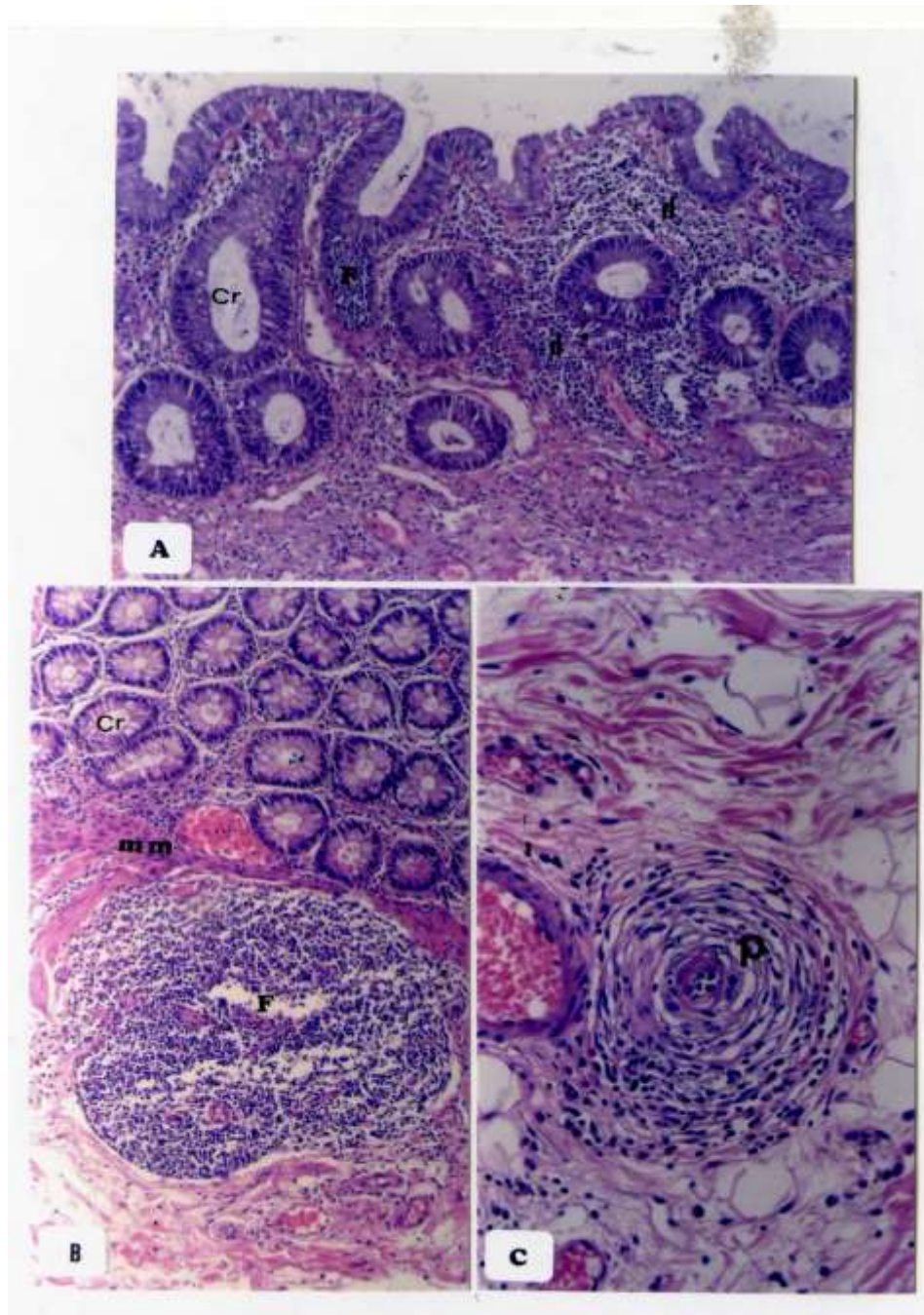


**Fig. (5):** Photomicrographs of sections in the human alimentary tract (*H&E X100*) showing: {**A**} mucosa of the appendix formed of crypts (Cr) , a large lymphatic follicle (F) and diffuse lymphocytes(d) are seen in the mucosa extending to the submucosa (*H&E, X100*), {**B**} the mucosa of the rectum with transversely cut crypts, muscularis mucosa (mm) and a solitary lymphatic follicle (F), {**C**} A Pacinian corpuscle (P) is seen close to a blood vessel in the submucosa.

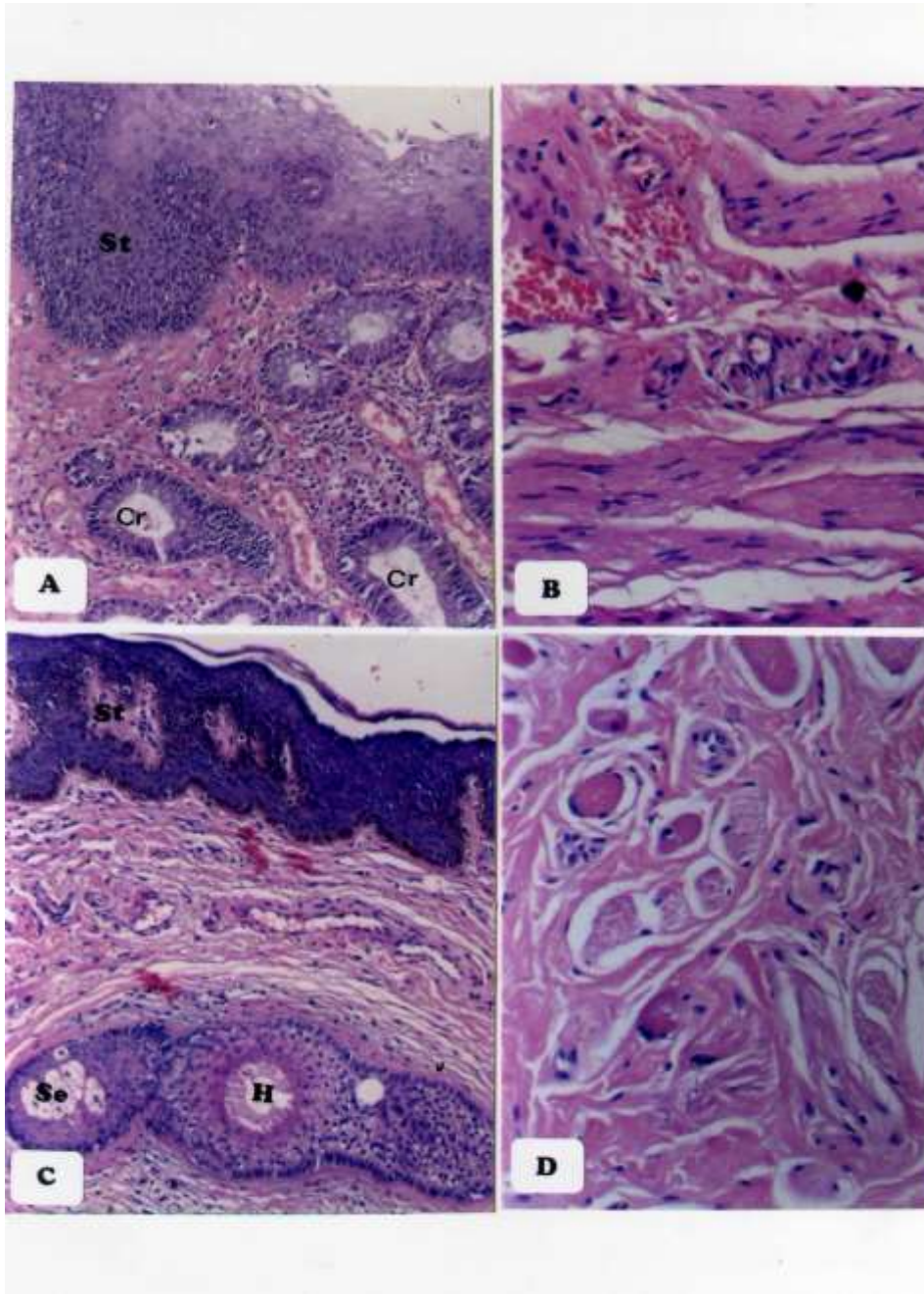


**Fig. (6):** Photomicrographs of sections in the human anal canal showing: **{A}** the mucosa at the recto-anal Junction is lined by stratified squamous epithelium (st) and crypts are seen (cr) (*H&E, X100*), **{B}** the internal anal sphincter formed of a thick layer of circular smooth muscle fibers (*H&E, X200*), **{C}** the skin covering the anal orifice with its epidermis being formed of keratinized stratified squamous epithelium (St). Dermis was formed of loose connective tissue rich in blood vessels with a sebaceous gland (Se) and a hair follicle (H) cut transversly (*H&E, X100*), **{D}** External anal sphincter formed of striated muscle fibers separated by connective tissue septa (*H&E, X200*).

### **Immunohistochemical results**

The c-kit positive cells were recognized as being ICC and mast cells. Differentiation was based on their morphology and location. C-kit positive mast cells could be demonstrated mainly in the mucosa and submucosa of the alimentary tract. Mast cells appeared as rounded cells with rounded nuclei, mostly located around the blood vessels (Fig.7A&B). On the other hand, ICC could be demonstrated at the level of the muscularis externa and showed two morphological patterns. Some appeared spindle-shaped with bipolar dendritic processes (Fig 8, A), while others were stellate-shaped with multiple cytoplasmic processes anastomosing with the processes of the adjacent ICC (Fig 8, B).

○At all levels of the esophagus, spindle-shaped ICC were seen around the myenteric plexus (Fig.9, A), but not at the level of submucosal plexus (Fig.9,B). Intramuscular ICC inbetween striated muscle fibers (Fig.9,C) and smooth muscle fibers (Fig.9,D) were observed. In the stomach, gastric fundus, corpus and pylorus showed different patterns of ICC distribution. ICC could not be demonstrated at the submucosal plexus at any level of stomach (Fig.10,A). In the fundus, myenteric plexus did not exhibit any positive immunoreaction (Fig.10,B). However, c-kit positive spindle ICC could be seen scattered inbetween the smooth muscle fibers of fundus (Fig.10,C). In the corpus, c-kit positive stellate-shaped ICC were noticed around the myenteric plexus (Fig.11,A), whereas, intramuscularly they appeared spindle-shaped (Fig.11,B). In the pylorus, c-kit positive spindle-shaped ICC could be demonstrated at the submucosal

border of the circular muscle layer (Fig.12,A). Multipolar c-kit positive ICC were noticed at the level of myenteric plexus (Fig.12,B). Intramuscular spindle ICC were seen inbetween the smooth muscle fibers (Fig.12,C). As for the small intestine, the duodenum, jejunum, and ileum revealed a similar pattern of ICC distribution. Multipolar c-kit immunoreactive ICC were demonstrated in two regions; the deep muscular plexus (between the thin inner and thick outer regions of the circular muscle layer) and encircling the myenteric plexus (Figs. 13 & 14). In the cecum, appendix, and colon the submucosal plexus did not exhibit any positive ICC immunostaining (Fig.15,A). However, c-kit positive spindle shaped ICC were seen at the submucosal border of the circular muscle layer (Fig.15,B). Intramuscular c-kit positive multipolar ICC could be demonstrated within the smooth muscle layer (Fig.15,C). C-kit positive multipolar ICC were also noticed encasing the myenteric plexus (Fig.16). In the rectum, c-kit positive spindle-shaped ICC were demonstrated at the submucosal border of the circular muscle layer (Fig.17,A). Another group of stellate multipolar ICC were seen at the level of the myenteric plexus. (Fig.17,B). Intramuscular spindle-shaped ICC were present inbetween the smooth muscle fibers (Fig.17,C). As for the anal canal, c-kit positive spindle ICC were demonstrated inbetween smooth muscle fibers of the internal anal sphincter (Fig.18,A). However, c-kit positive ICC could not be observed inbetween striated muscle fibers of external anal sphincter (Fig. 18,B).

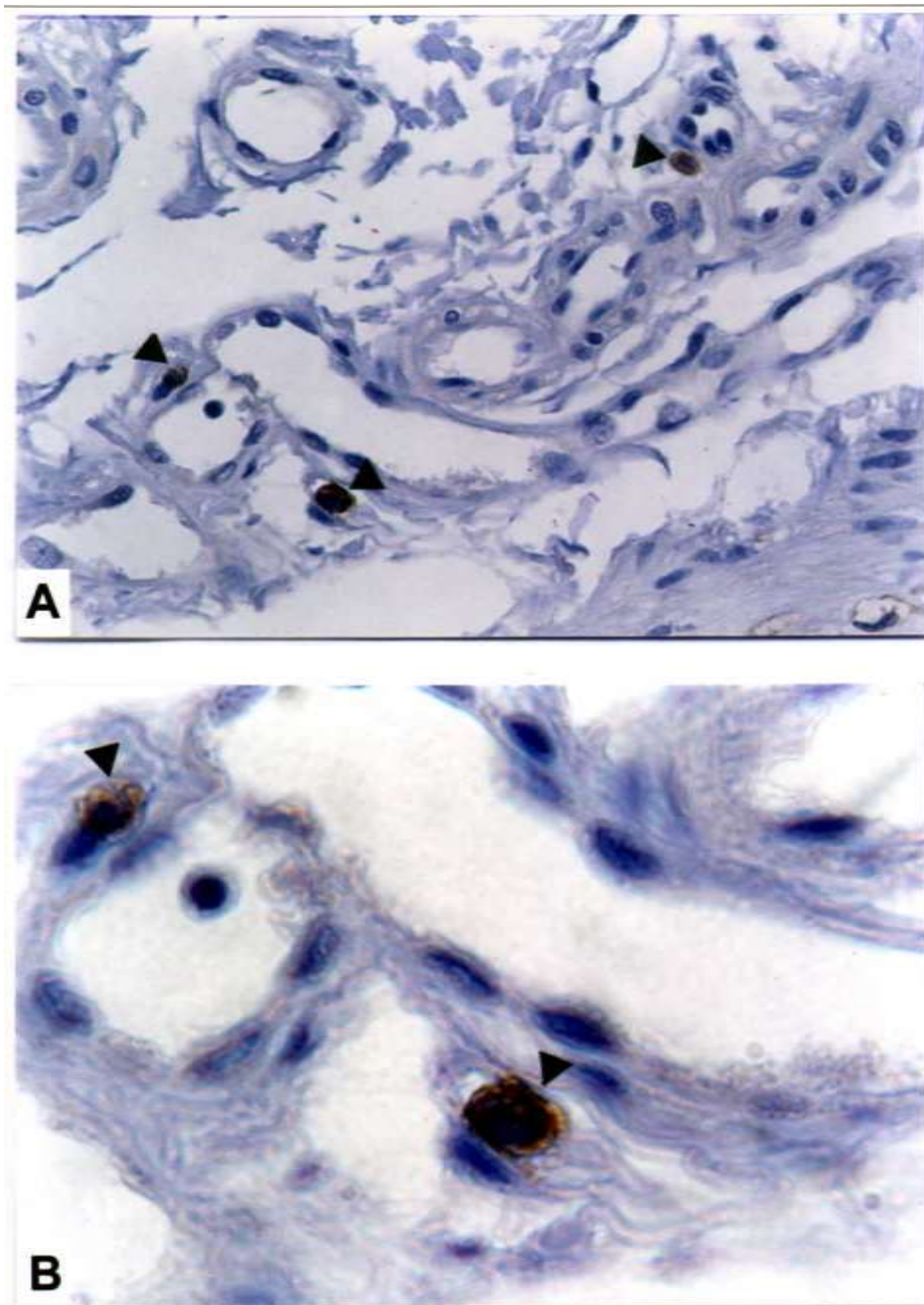


**Fig.(7):** Photomicrographs of a section in the human colon (*c-kit immunostaining*) revealing: **{A}** positively stained mast cells (arrow heads) in the submucosa close to a blood vessel (*X400*),**{B}** higher magnification of the previous photomicrograph showing positively stained mast cells (arrow heads) which appear as rounded cells with rounded nuclei (*X1000*).

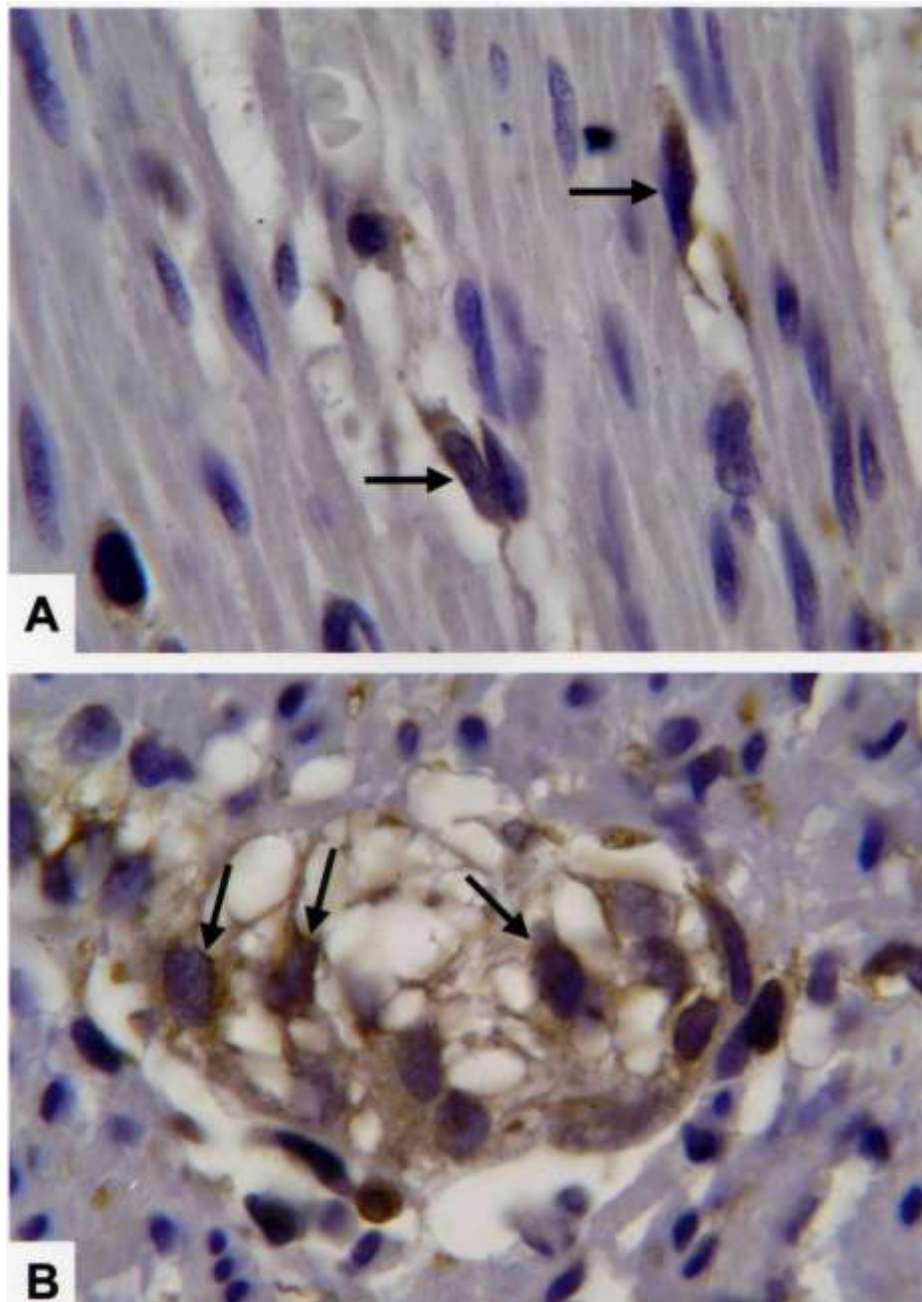


**Fig. (8):** Photomicrographs of sections in the human colon (*c-kit* immunostaining, X1000) revealing: {A} *c-kit* positive spindle shaped ICC (arrows) inbetween smooth muscle fibers. {B} *c-kit* positive multipolar ICC (arrows) at the level of myenteric plexus.

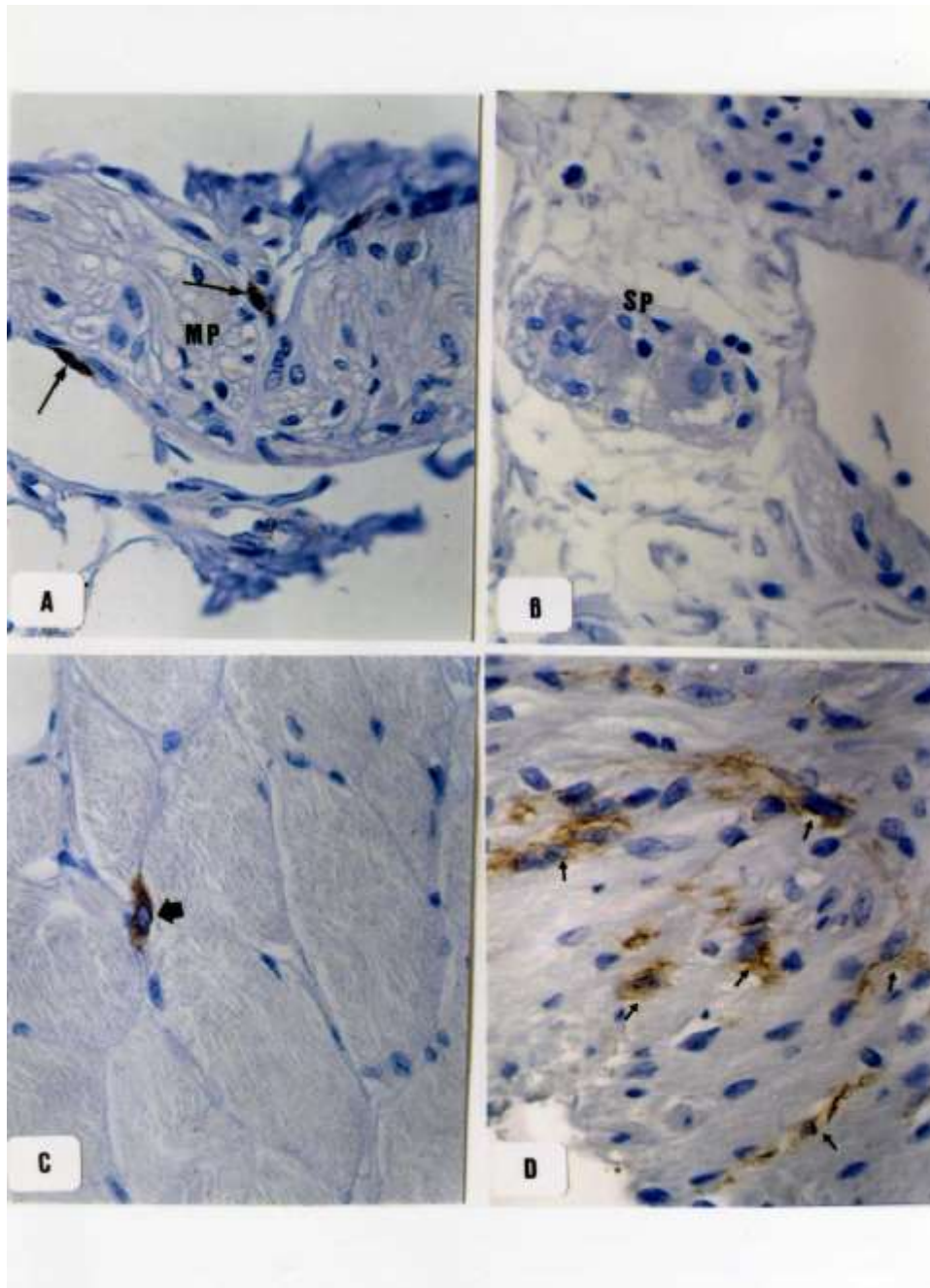


**Fig. (9):** Photomicrographs of sections in the human esophagus (*c-kit Immunostaining, X400*) revealing: **{A}** c-kit positive ICC (arrows) at the level of the myenteric plexus (MP). ICC appear as spindle-shaped cells with prominent oval nuclei, **{B}** negative ICC expression at the submucosal plexus (SP), **{C}** c-kit positive spindle-shaped ICC with bilateral processes (arrow) enclosed within the striated muscle fibers, **{D}** multiple c-kit positive spindle ICC (arrows) scattered within the smooth muscle layer.

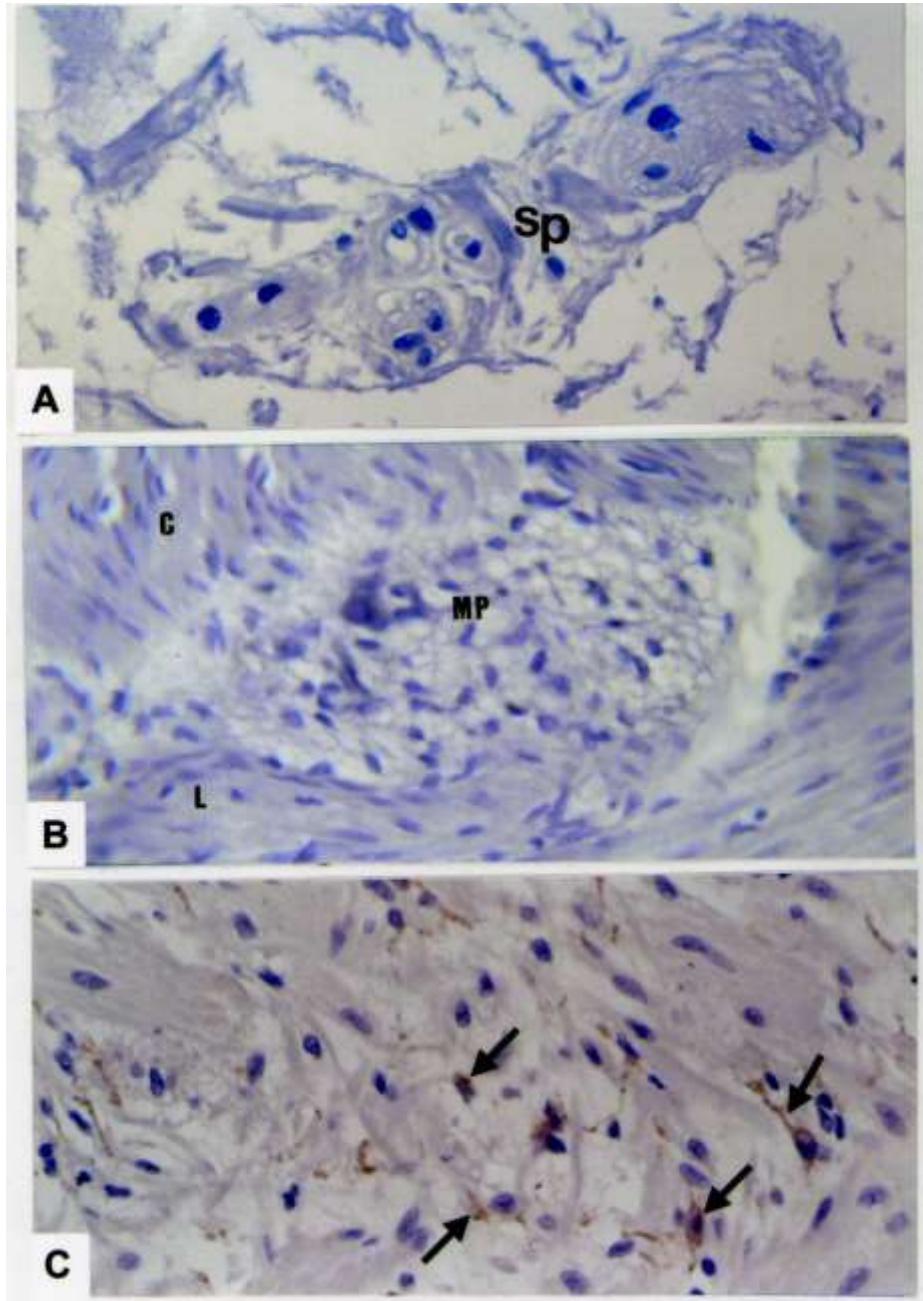


**Fig.(10):** Photomicrographs of sections in the human fundus (*c-kit immunostaining, X400*) revealing: {**A**} negative immunoreaction at the submucosal plexus (SP), {**B**} negative immunoreaction at the myenteric plexus (MP) in the plane between the circular and the longitudinal (L) muscle layers,{**C**} positively stained spindle ICC with bilateral processes scattered between smooth muscle fibers (arrows).

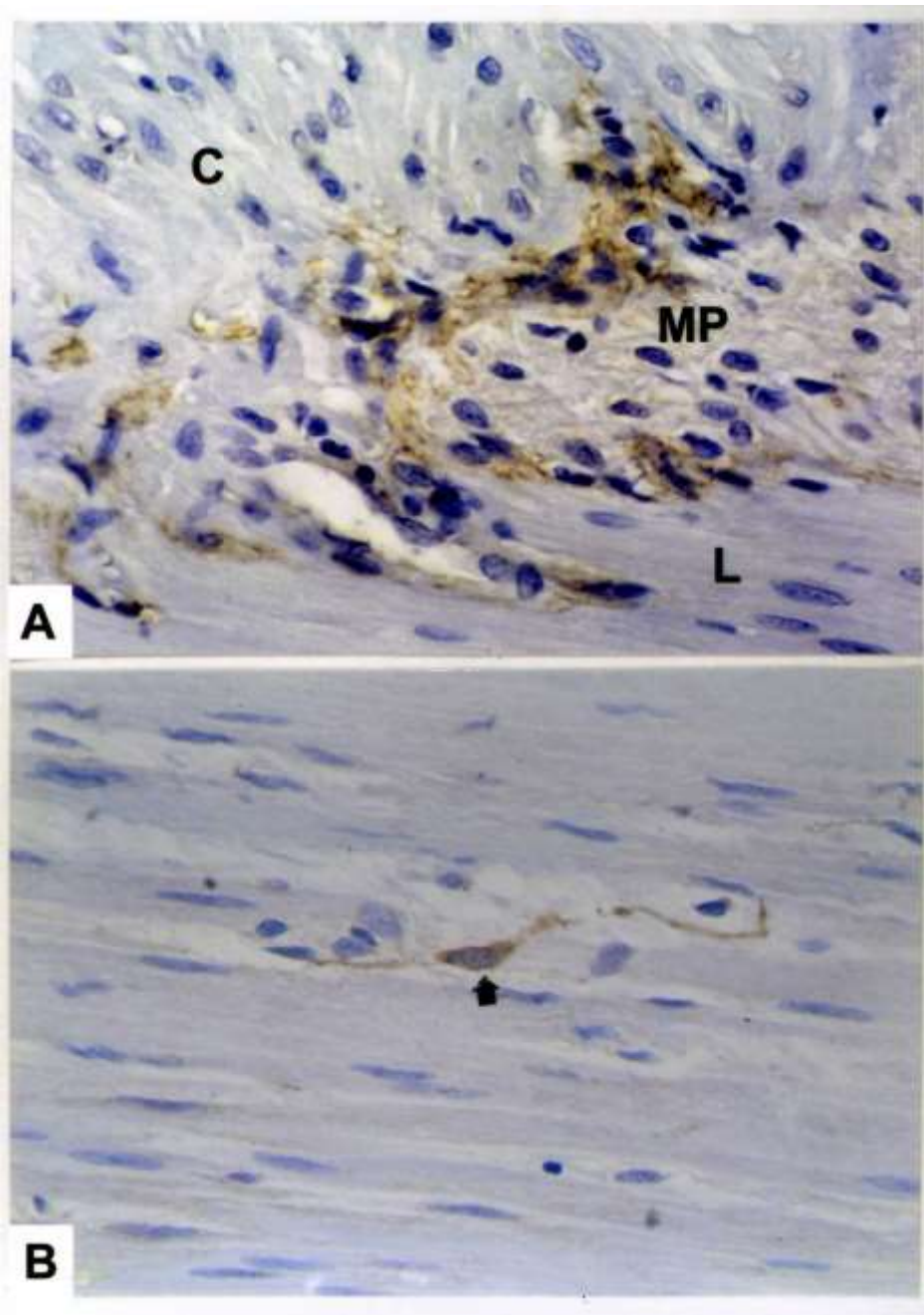


**Fig.(11):** Photomicrographs of sections in the human corpus (*c-kit Immunostaining, X400*) showing: {**A**} *c-kit* positive stellate-shaped ICC around the myenteric plexus (MP) in the plane between the circular (C) and the longitudinal (L) muscle layers, {**B**} *c-kit* positive spindle ICC (arrow) inbetween longitudinal muscle fibers.

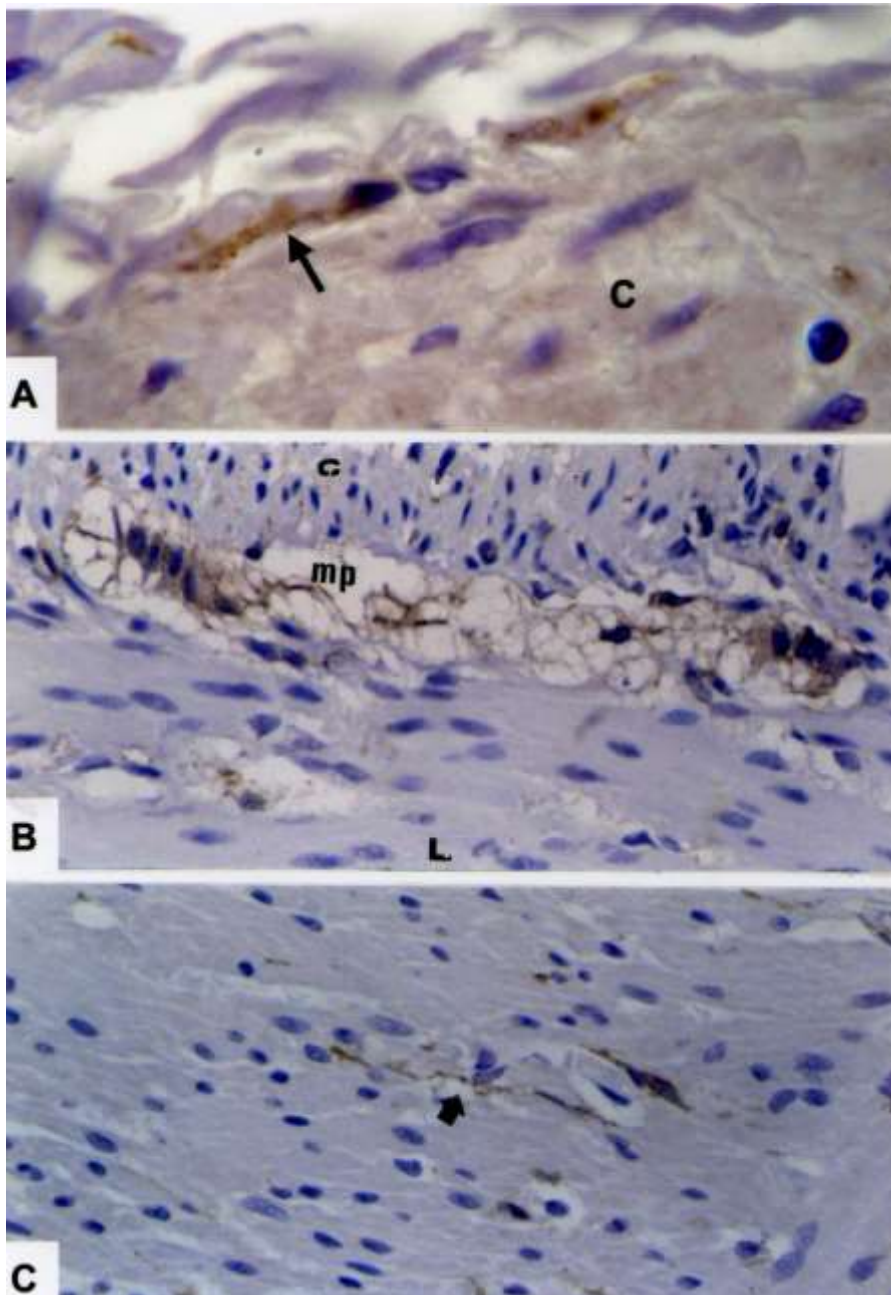


**Fig.(12):** Photomicrographs of a section in the human pylorus (*c-kit immunostaining*) showing: {**A**} *c-kit* positive spindle-shaped ICC (arrow) at the submucosal border of the circular muscle layer (C) (*X1000*), {**B**} multipolar *c-kit* positive ICC at the myenteric plexus (mp) inbetween circular (C) and longitudinal (L) muscle layers (*X400*), {**C**} spindle *c-kit* positive ICC (arrow) inbetween smooth muscle fibers (*X400*).

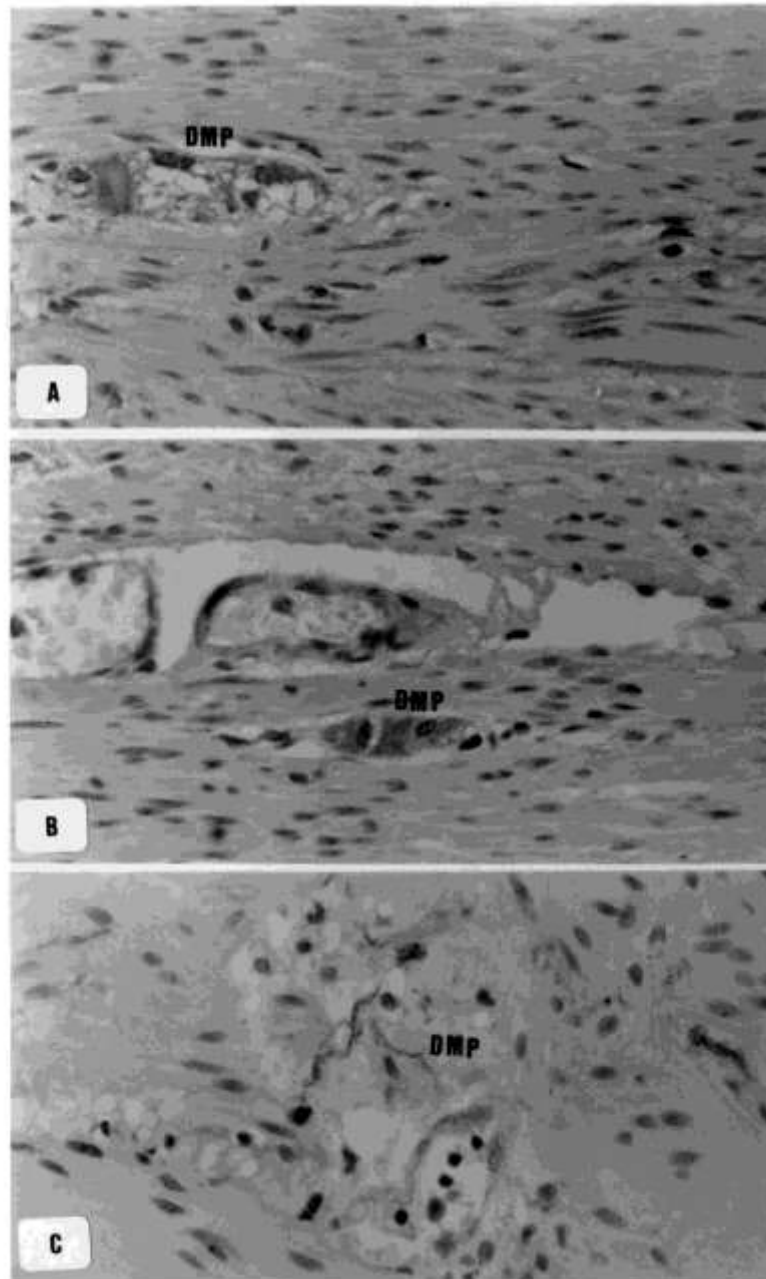


**Fig.(13):** Photomicrographs of sections in the human small intestine (*c-kit* immunostaining, X400) revealing: multipolar positively-stained ICC at the level of the deep muscular plexuses (DMP) within the circular muscle layer of the {A} duodenum, {B} jejunum & {C} ileum. Notice the prominent oval nuclei and the extending cytoplasmic processes of ICC.

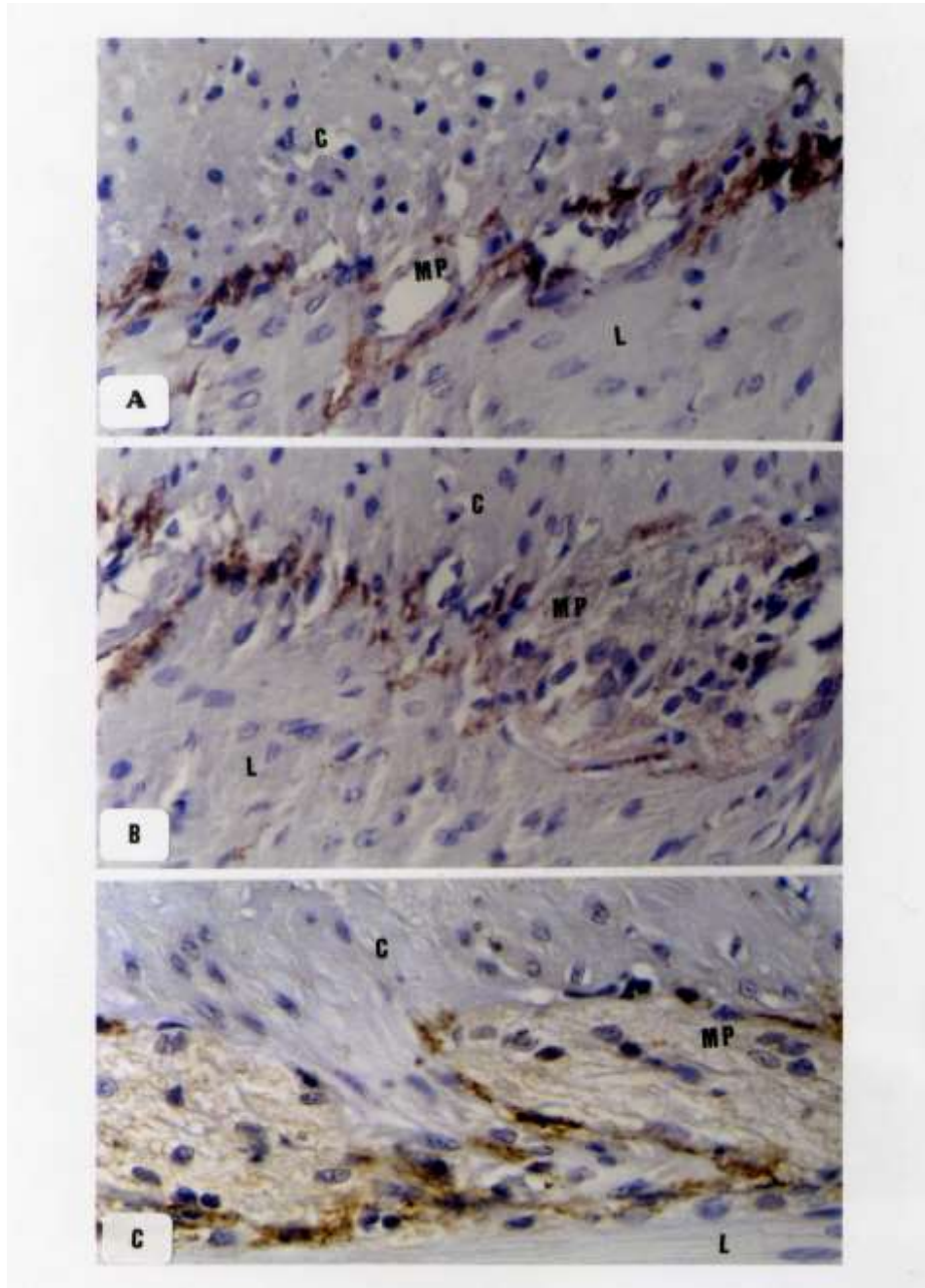


**Fig.(14):** Photomicrographs of sections in the human small intestine (*c-kit* Immunostaining, X400) revealing positively-stained ICC encasing the myenteric plexus (MP) between circular (C) and longitudinal (L) muscle layers, {A} in duodenum, {B} in jejunum and {C} in ileum.

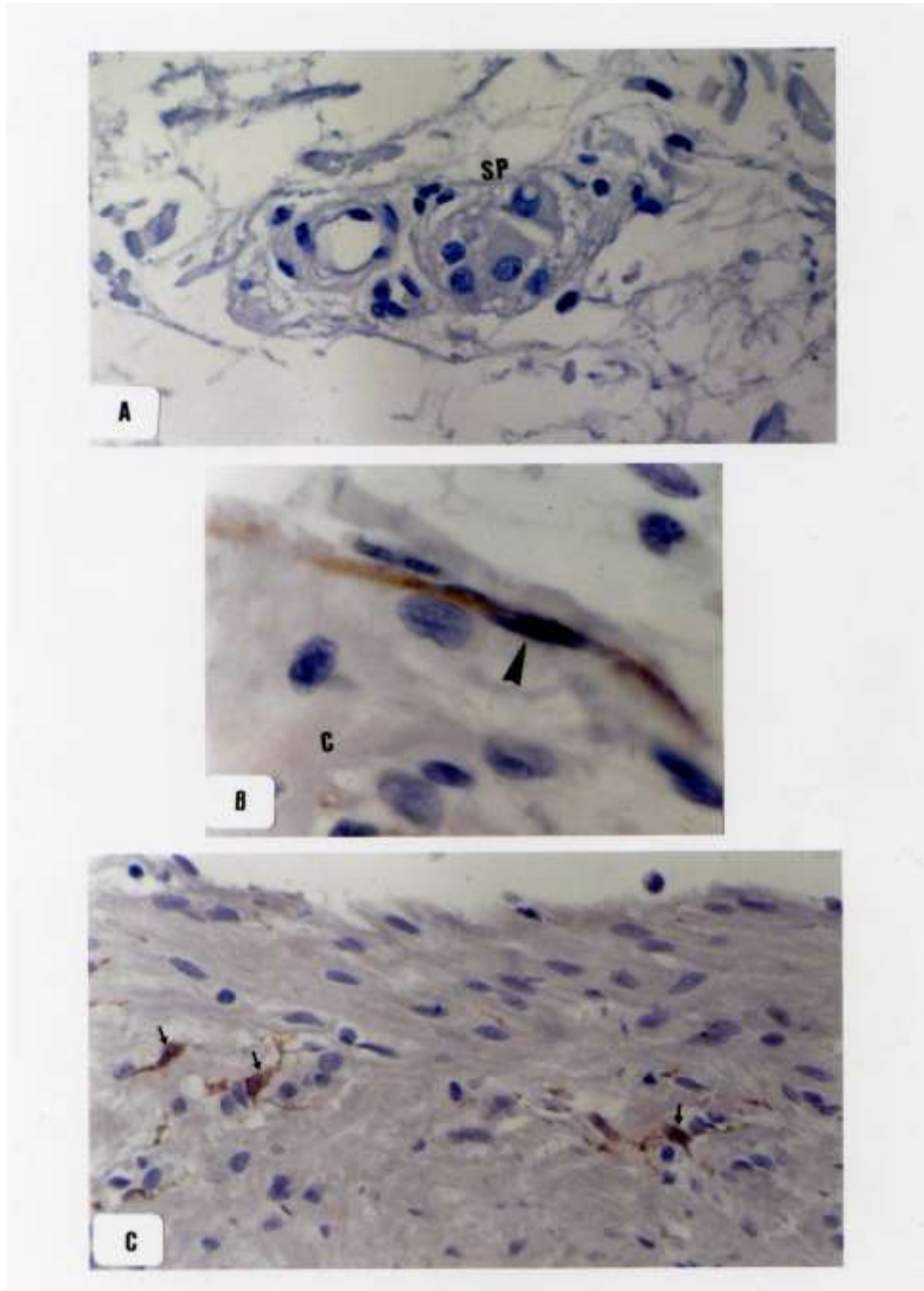


**Fig.(15):** Photomicrographs of sections in human ascending colon (*c-kit immunostaining*) revealing: **{A}** a submucosal plexus (SP) with no detected immunostained ICC (X400), **{B}** positively stained spindle shaped ICC (arrow head) with bilateral processes at the submucosal border of the circular muscle layer (C) (X1000), **{C}** positively immunostained multipolar ICC (arrows) within the circular muscle layer (X400).

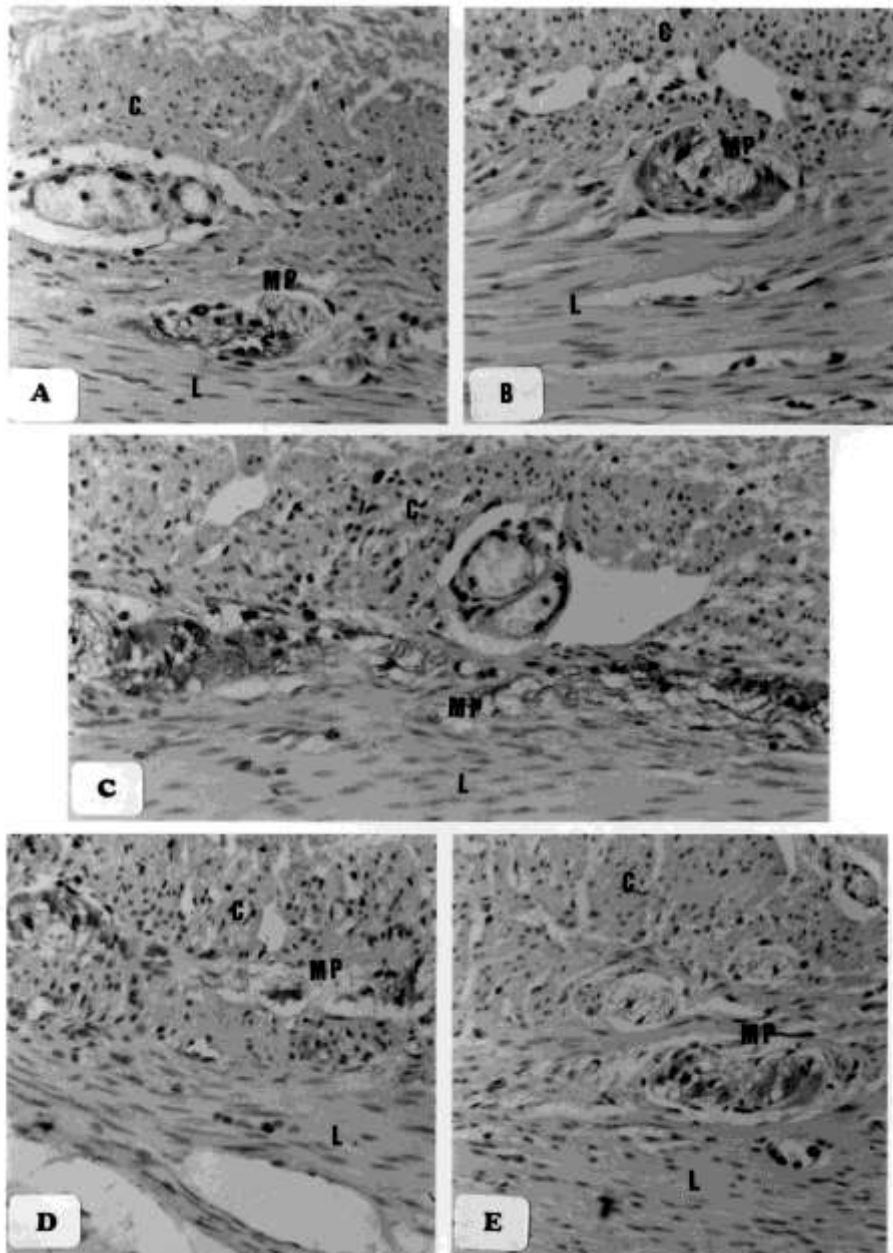


**Fig.(16):** Photomicrographs of sections in the human colon (*c-kit* immunostaining, X200) showing positively-stained ICC at the level of the myenteric plexus (MP) in the {A} cecum, {B} ascending colon, {C} transverse colon, {D} descending colon {E} appendix. ICC appeared as branched cells with multiple cytoplasmic processes extending in all directions and anastomosing with those of the adjacent ICC.

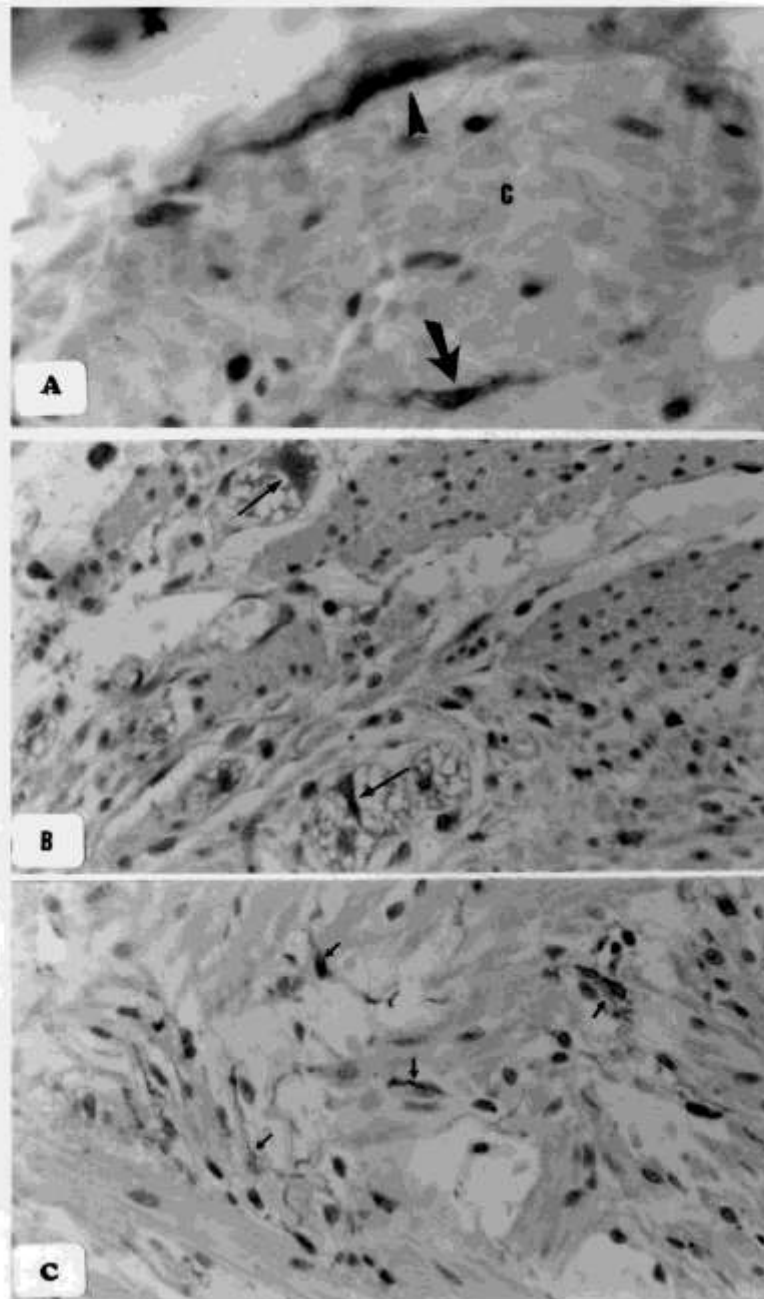


**Fig.(17):** Photomicrographs of sections in the human rectum (*c-kit immunostaining*) revealing: {**A**} a positively stained spindle-shaped ICC (arrow head) at the submucosal border of the circular muscle layer (C). Another ICC (arrow) is also observed within the circular muscle fibers (*X1000*), {**B**} *c-kit* positive multipolar ICC (arrows) with large oval nuclei are seen at the level of the myenteric plexus (*X400*), {**C**} positively immunostained ICC (arrows) in the outer longitudinal muscle layer (*X400*).

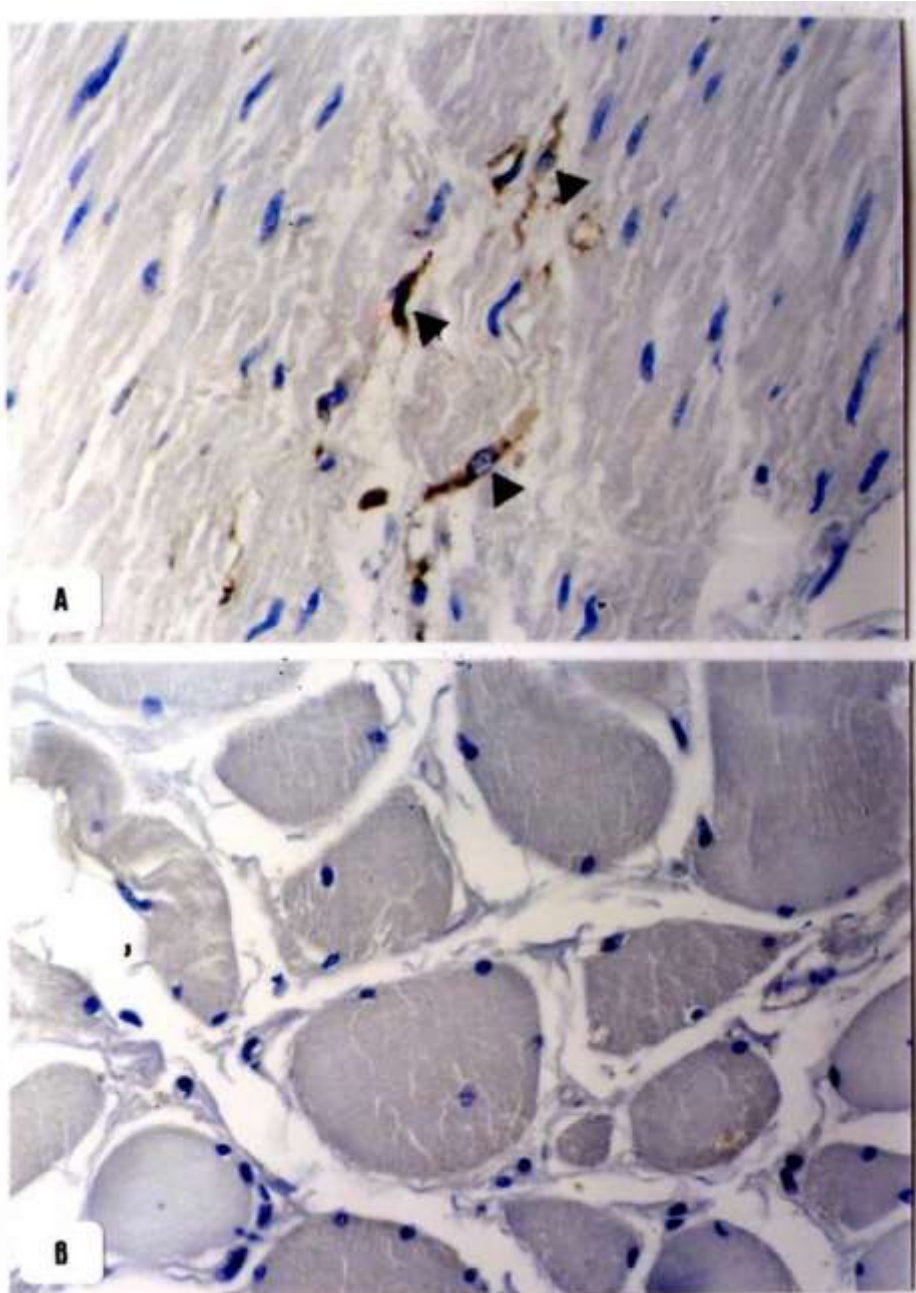


**Fig.(18):** Photomicrographs of sections in the human anal canal (*c-kit Immunostaining, X400*) revealing: **{A}** positively stained spindle-shaped ICC (arrow heads) within the smooth muscle layer of the internal anal sphincter, **{B}** negative immunostaining for ICC in the striated muscle layer of the external anal sphincter.

### QuantitativeMorphometric Results:

**In the esophagus**, regarding the transmural distribution of immunoreactivity, as shown in table 2, the mean area percent of myenteric plexus ICC in the upper and middle levels was higher than that of intramuscular ICC but the difference was statistically significant only at upper level. In the lower esophagus, the mean area percent of intramuscular ICC was higher than that of myenteric plexus ICC but the difference was statistically insignificant. As for the regional

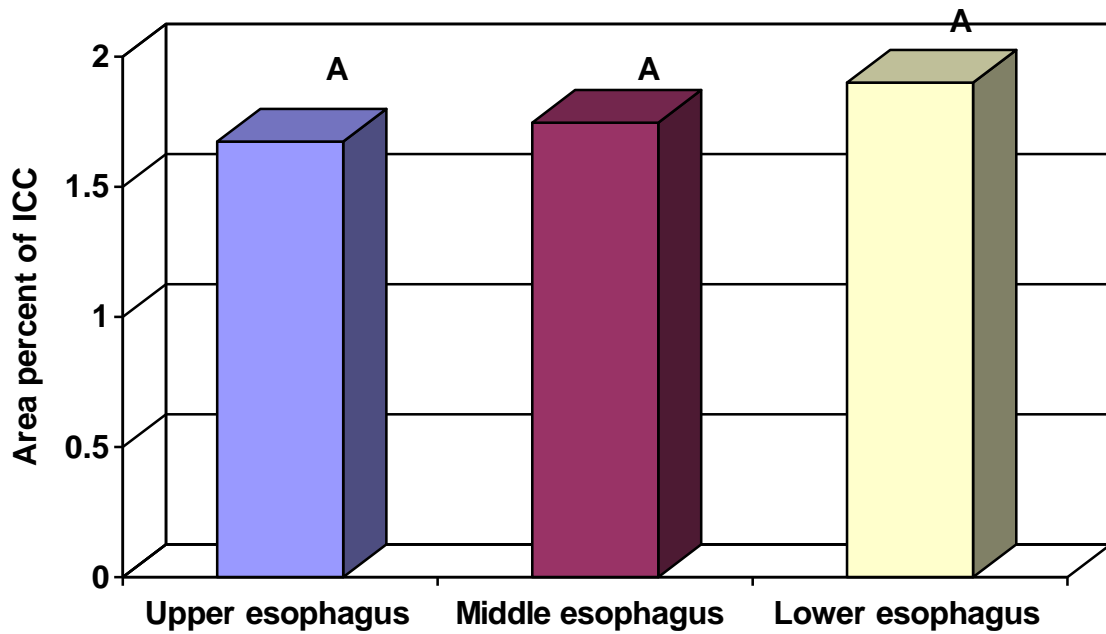
distribution, at the level of myenteric plexus ICC the mean area percent of positive immunoreactivity was maximum in the lower esophagus but the difference was statistically insignificant (Fig.19). At the level of intramuscular ICC, the highest mean area percent was also reported in the lower esophagus which was statistically significantly higher than that of upper esophagus but no statistically significant difference was found comparing middle and lower segments of esophagus (Fig.20).

**Table 2. Comparison of the mean area percent of ICC present in the different segments of esophagus.**

	ICC Mean $\pm$ SD		P value
	Myenteric plexus	Intramuscular	
<i>Upper esophagus</i>	1.674 $\pm$ 0.748	0.832 $\pm$ 0.335	0.004*
<i>Middle esophagus</i>	1.746 $\pm$ 0.868	1.732 $\pm$ 0.757	0.9
<i>Lower esophagus</i>	1.9 $\pm$ 0.726	2.298 $\pm$ 0.964	0.31

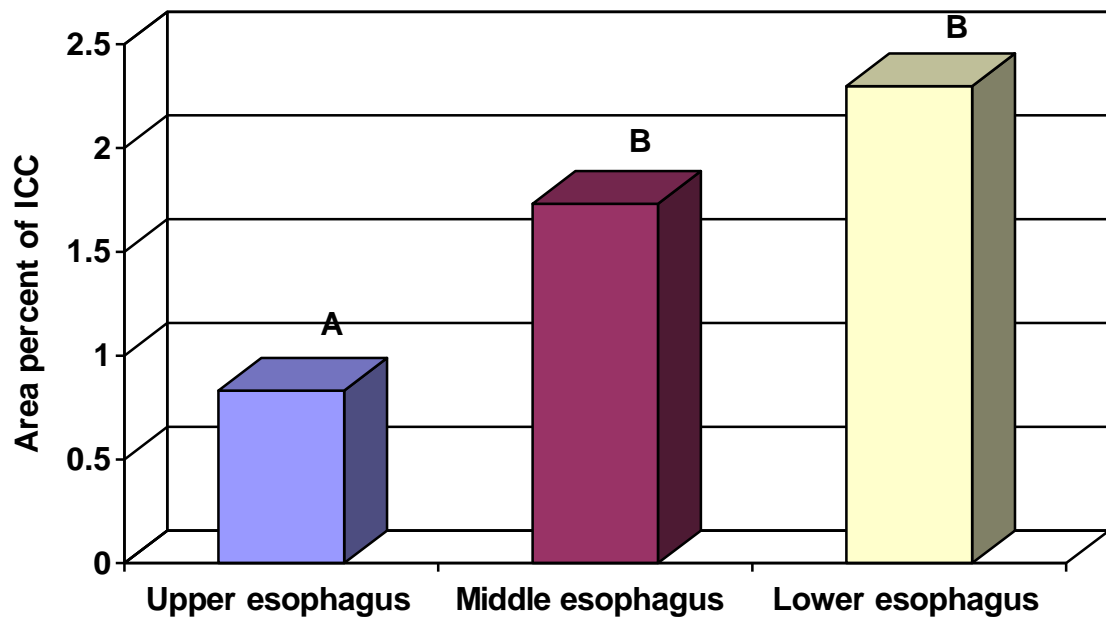
\* significant difference ( $P < 0.05$ )

**Fig. (19): Mean area percent of myenteric plexus ICC in different segments of esophagus.**



\*No statistical significant difference between segments sharing the same letter.

**Fig. (20): Mean area percent of intramuscular ICC in different segments of esophagus.**



\*Segments sharing the same letter are not statistically significant from each other at  $p \leq 0.05$ .

**In the stomach**, transmural immunoreactivity (Table 3) revealed that in the fundus, ICC were only observed intramuscularly. In the corpus, the mean area percent of myenteric plexus ICC was higher than that of intramuscular ICC and the difference was found to be statistically significant. However, in the pylorus, the mean area percent of myenteric plexus ICC was higher than those of both submucosal and intramuscular ICC and the difference reached the level of statistical significance.

Regarding the regional distribution, the mean area percent of myenteric plexus ICC in the pylorus was higher than that of the corpus and the difference was statistically significant (Fig.21). There were no myenteric plexus ICC in fundus. On the other hand, the mean area percent of intramuscular ICC was highest in the fundus and decreased towards the pylorus but the difference was statistically insignificant (Fig.22). Submucosal ICC was restricted only to the pylorus.

**Table (3): Comparison of the mean area percent of ICC in the different segments of stomach.**

	ICC Mean±SD			P value		
	Submucosal	Myenteric plexus	Intramuscular	P1	P2	P3
<b>Fundus</b>	0	0	2.331±1.239			
<b>Corpus</b>	0	4.976±1.695	1.9±0.726	0.00005*		
<b>pylorus</b>	1.746±0.868	6.515±1.327	1.674±0.748	0.00000*	0.00001*	0.84

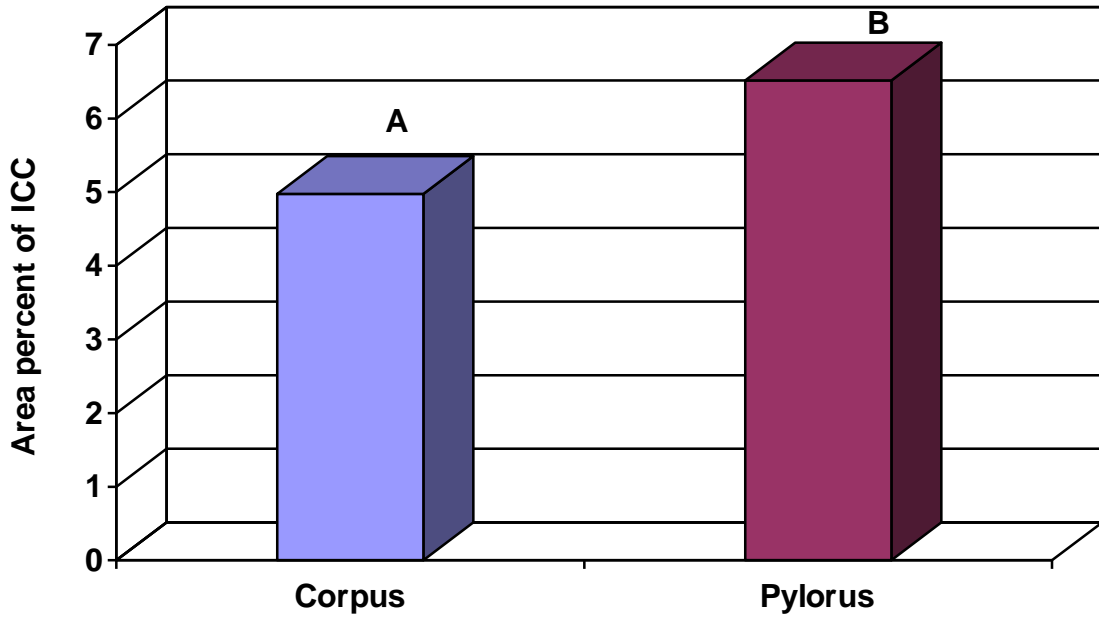
*P1 : myenteric plexus ICC versus intramuscular ICC*

*P2 : submucosal ICC versus myenteric plexus ICC*

*P3 : submucosal ICC versus intramuscular ICC*

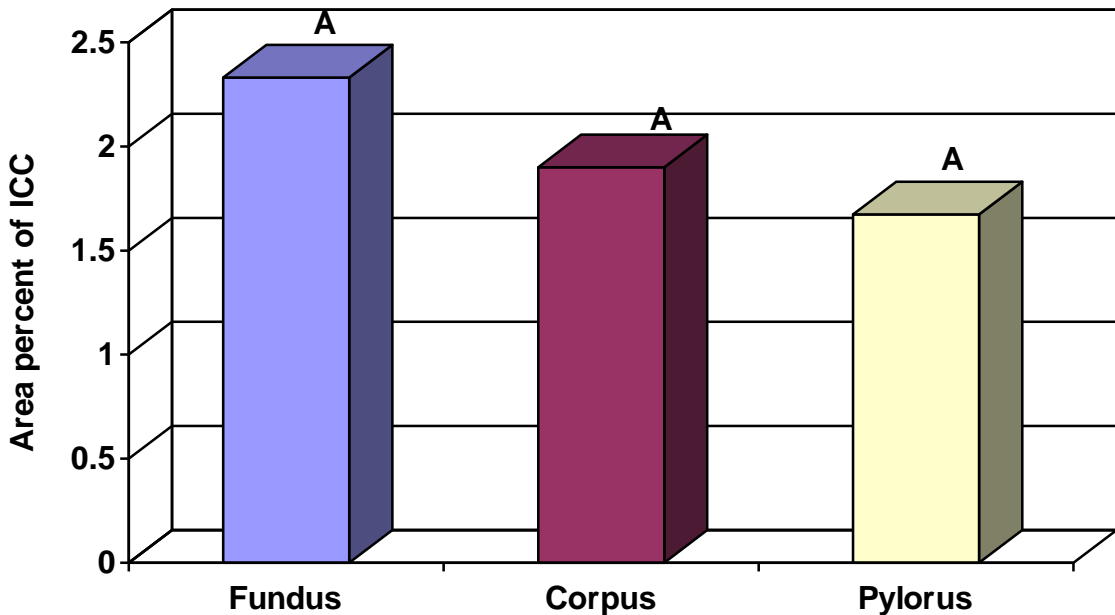
*\* : significant difference (P < 0.05)*

**Fig. (21): Mean area percent of myenteric plexus ICC in different segments of stomach.**



\*Segments sharing the same letter are not statistically significant from each other.

**Fig. (22): Mean area percent of intramuscular ICC in different segments of stomach.**



\*No statistical significant difference between segments sharing the same letter.

Concerning the small intestine, in all the segments the transmural distribution of immuoreactivity revealed that the mean area percent of myenteric plexus ICC was higher than that of deep muscular plexus ICC and the difference was statistically significant (table 4). As for the regional distribution of

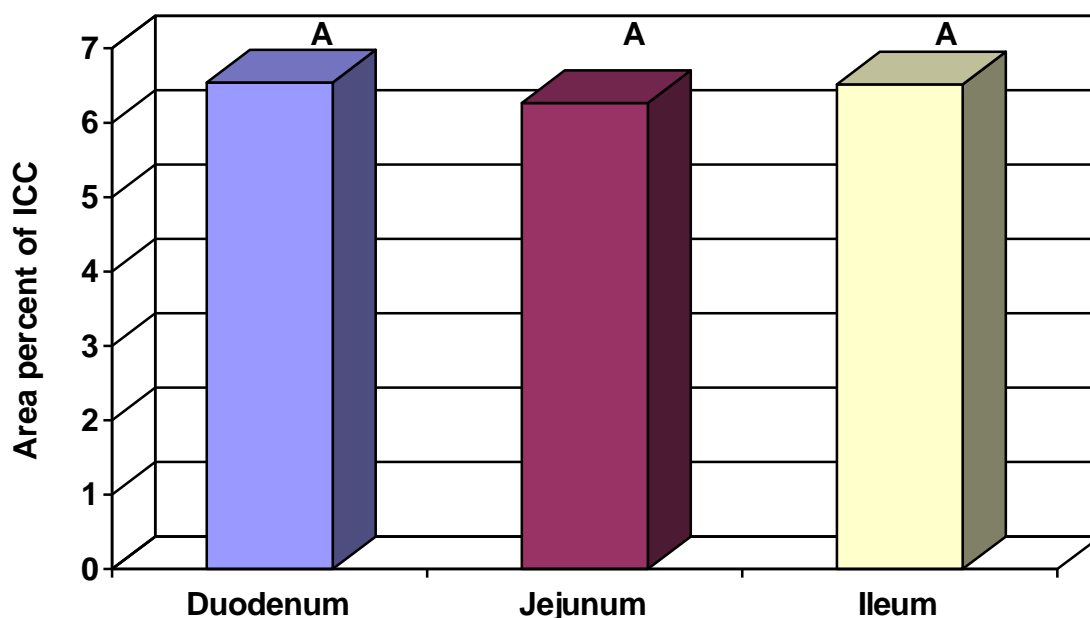
immunoreactivity, the highest mean area percent of myenteric plexus ICC was reported at the duodenum (Fig.23). At the level of deep muscular plexus ICC, the highest mean area percent was observed at the jejunum (Fig.24). However, both differences were statistically insignificant.

**Table (4): Comparison of the mean area percent of ICC in the different segments of smal intestine.**

	ICC Mean±SD		P value
	Myenteric plexus	Deep muscular plexus	
<i>Duodenum</i>	6.54±1.892	2.298±0.964	0.00000*
<i>Jejunum</i>	6.265±2.784	2.331±1.239	0.0007*
<i>Ileum</i>	6.515±1.326	2.091±0.536	0.00000*

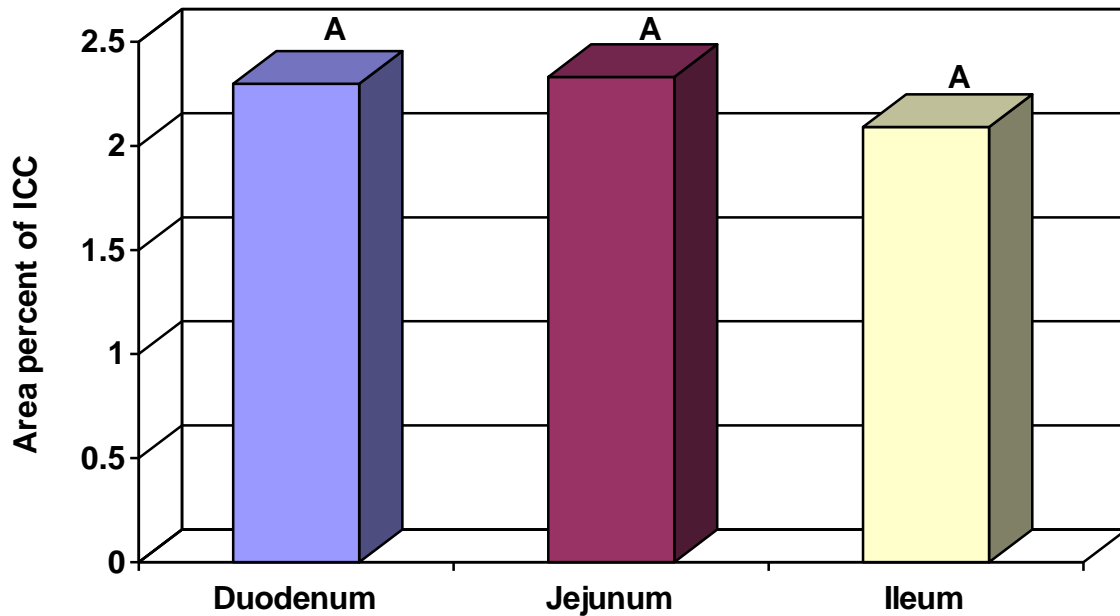
\* : significant difference ( $P < 0.05$ )

**Fig. (23): Mean area percent of myenteric plexus ICC in different segments of small intestine.**



\*No statistical significant difference between segments sharing the same letter.

**Fig. (24): Mean area percent of deep muscular plexus ICC in different segments of small intestine.**



\*No statistical significant difference between segments sharing the same letter.

**Regarding the Large intestine,** the transmural distribution of immunoreactivity (Table 5) showed that in all levels the myenteric plexus ICC showed the highest mean area percent followed by intramuscular ICC and the lowest levels were observed in the submucosal ICC. Comparing the mean area percent of myenteric plexus ICC to submucosal ICC, the differences were found to be statistically significant at all levels. On the other hand, comparing the mean area percent of myenteric plexus ICC to intramuscular ICC, the differences were found to be statistically significant in all levels of the large intestine except in the appendix and the rectum. Comparing intramuscular ICC to submucosal ICC, level of statistical significance was only reached in the appendix and the rectum.

The regional distribution of immunoreactivity revealed that at the level of submucosal ICC, the highest mean area percent was reported at transverse colon

but the difference was statistically significant only when comparing it with that of the appendix, however, level of statistical significance was not reached when compared to the other colonic regions (Fig. 25). At the level of myenteric plexus ICC, the highest mean area percent was also observed at the transverse colon. This was found to be statistically significant when compared only to that of the cecum, appendix and ascending colon (Fig. 26). As for intramuscular ICC, the highest mean area percent was reported at the rectum, followed by the anal canal. The mean area percent of both was much higher than that in all other colonic regions and was found to be statistically significant when compared to them. However, comparing the mean area percent of intramuscular ICC in the rectum to that of the anal canal was found to be statistically insignificant (Fig.27).

**Table 5. Comparison of the mean area percent of ICC in the different segments of large intestine.**

	ICC Mean±SD			P value		
	Submucosal	Myenteric plexus	Intramuscular	P1	P2	P3
<i>Cecum</i>	1.674±0.748	4.976±1.695	2.091±0.536	0.000*	0.16	0.000*
<i>Appendix</i>	0.832±0.335	2.331±1.239	1.674±0.748	0.001*	0.004*	0.16
<i>Ascending colon</i>	1.746±0.868	5.244±1.745	2.298±0.964	0.000*	0.19	0.000*
<i>colon</i>	1.9±0.726	7.987±2.531	2.331±1.239	0.000*	0.35	0.000*
<i>Descending colon</i>	1.746±0.868	6.265±2.784	2.298±0.964	0.000*	0.19	0.000*
<i>Rectum</i>	1.674±0.748	6.54±1.892	6.265±2.784	0.000*	0.000*	0.79
<i>Anal canal</i>	0	0	4.976±1.695			

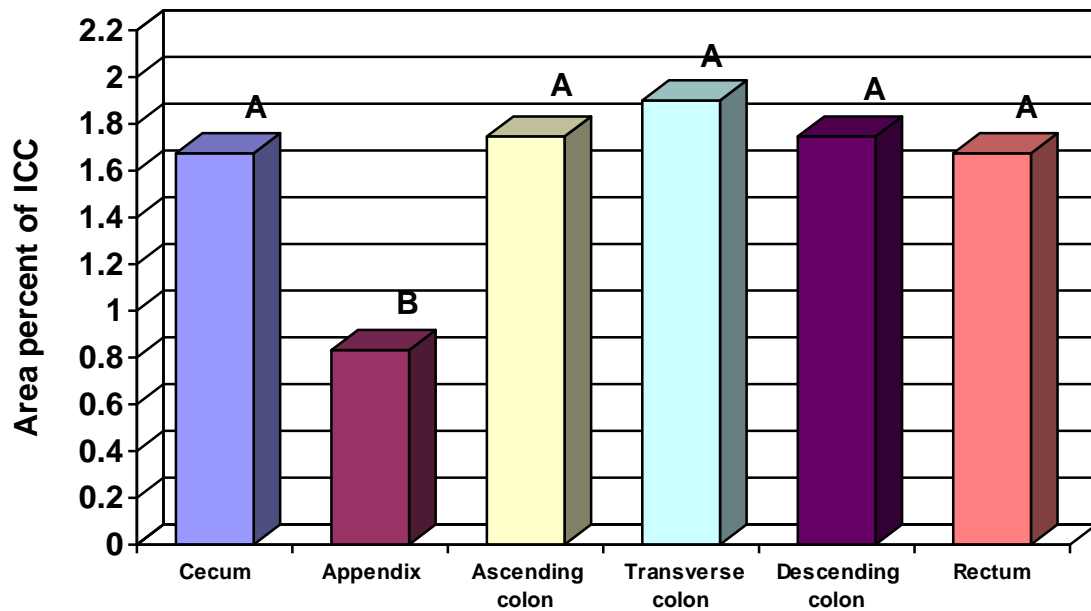
*P1* : submucosal ICC versus myenteric plexus ICC

*P2* : submucosal ICC versus intramuscular ICC

*P3* : myenteric plexus ICC versus intramuscular ICC

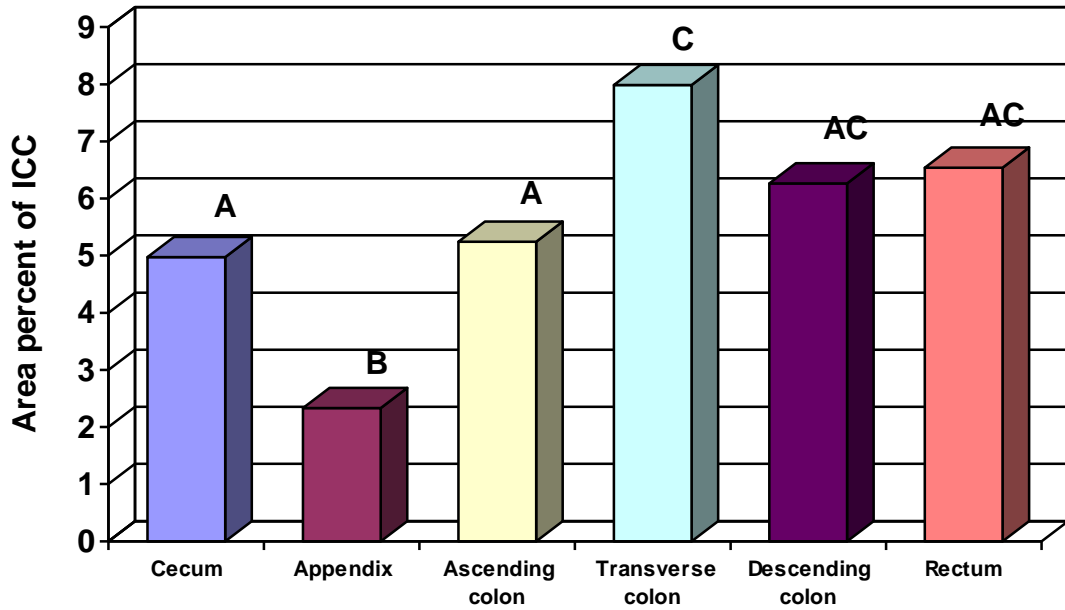
\* : significant difference ( $P < 0.05$ )

**Fig. (25): Mean area percent of submucosal ICC in different segments of large intestine.**



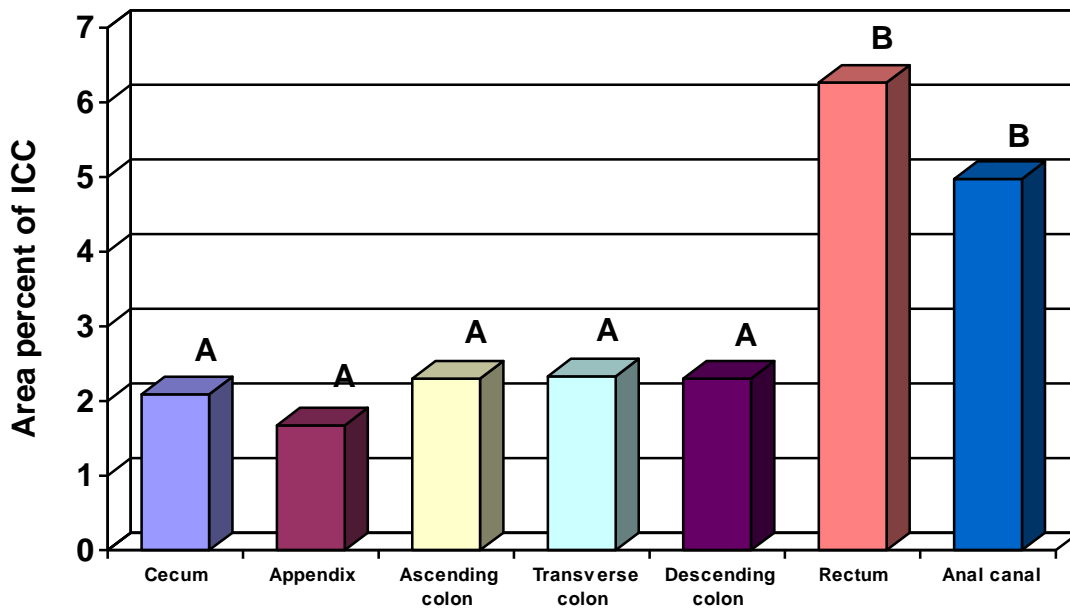
\*Segments sharing the same letter are not statistically significant from each other at  $p \leq 0.05$ .

**Fig. (26): Mean area percent of myenteric plexus ICC in different segments of large intestine.**



\*Segments sharing a letter are not significantly different from each other at  $p \leq 0.05$ .

**Fig. (27): Mean area percent of intramuscular ICC in different segments of large intestine.**



\*Segments sharing the same letter are not significantly different from each other at  $p \leq 0.05$ .

## DISCUSSION

Interstitial cells of Cajal (ICC) refer to a group of cells located in the musculature of the alimentary tract. Some ICC groups act as sources of spontaneous, electric slow waves responsible for paced contractions “pacemaker”, whereas other ICC groups are involved in the modulation of enteric neurotransmission (**Huizinga *et al.*,1998**). Moreover, a wide variety of gut motility disorders has been postulated to have a direct relation to ICC (**Vanderwinden *et al.*,1996**). In the present work, ICC could not be demonstrated by the routine hematoxylin and eosin stain. The same finding was documented by **Hagger *et al.*(1998)**. Thus, immunohistochemical staining with c-kit antibody was done to detect the distribution of c-kit positive ICC in the different segments of the alimentary tract. **Kindblom *et al.*, (1998)** reported the efficiency of immunohistochemistry in studying the c-kit positive ICC in gastrointestinal tissues. In the present study, immunohistochemistry using the c-kit antibody identified, on a morphological basis, two different cell types in the alimentary tract which have positively expressed c-kit, the ICC and mast cells. The c-kit positive cells which appeared as rounded cells, mostly located around blood vessels mainly in the mucosa and submucosa were believed to be mast cells. This was in agreement with the previous finding of **Vanderwinden *et al.*(1996)** who suggested a developmental role for the c-kit in these cells. The morphological characteristics of ICC, reported in the current work, would suggest the subclassification of these cells into two categories, namely the spindle bipolar and the stellate multipolar forms. This was in accordance with those described in human and mouse (**Vanderwinden *et al.*,2000**) in a c-kit immunohistochemical study. Also, in 1999, **Hanani *et al.*** demonstrated the same two morphological types of ICC in freshly lipophilic dye-labeled ICC. They confirmed their finding by ultrastructural examination of these labeled cells. In 2005, **Nishitani *et al.*** documented the expression of connexin 43, a gap junction protein, in small intestinal GISTs but not in gastric GISTs. This observation would additionally

propose the existence of more than one functional variant of ICC. In the present work, the mean area percent of ICC in both myenteric plexus and intramuscular regions of the esophagus was higher in the lower segment than those of the upper and middle segments. The intramuscular condensation of ICC in the lower segment suggested that they could be important mediators of enteric inhibitory neurotransmission in the lower esophageal sphincter. In the upper and middle segments, the mean area percent of myenteric plexus ICC was higher than that of intramuscular ICC while it was reversed in the lower segment. Physiological studies have suggested that the areas of high density of ICC roughly correspond to the areas of prominent slow waves which represent pacemaker activity (**Christensen *et al.*, 1992**). The previous works of **Ward *et al.*(1998)**, **Rumessen *et al.*(2001)**, and **Wu *et al.*(2003)** demonstrated the presence of intramuscular ICC in the esophagus but did not report their presence in the myenteric plexus.. However, these studies were conducted on experimental animals while the current work studied human tissue. In the present study, only intramuscular ICC were detected in gastric fundus. Both myenteric plexus and intramuscular ICC were demonstrated in gastric corpus and pylorus. In gastric pylorus, an additional subtype of ICC was observed at the submucosal border of the circular muscle layer. The proportion of intramuscular ICC was highest in the fundus and myenteric plexus ICC were highest in the pylorus. These findings were consistent with the results of **Burns *et al.*(1997)** who studied ICC distribution in guinea pig stomach but submucosal ICC were not reported at the level of pylorus. **Vanderwinden *et al.*(2000)** reported ICC distribution in human and mouse stomach. They reported the presence of intramuscular ICC in both human and mouse corpus and pylorus, but myenteric plexus ICC were detected only in the pylorus. On the other hand, **Mazet and Raynier (2004)** reported the presence of myenteric plexus, intramuscular and submucosal ICC in guinea pig gastric antrum. **Manneschi *et al.*(2004)** reported

the presence of myenteric plexus and intramuscular ICC in human fundus, corpus, and antrum. From the previous studies, it appears that there was much controversy regarding the regional distribution of ICC in stomach. The fundus is not myogenically active (**Komori and Suzuki,1986**) and this might simply result from the absence of myenteric plexus ICC reported in the present work. In the fundus, intramuscular ICC mediate inhibitory and excitatory neurotransmissions in the circular muscle layer (**Burns et al.,1996**). In the pylorus, the primary component of each slow wave is initiated by myenteric plexus ICC. The passive wave of pacemaker depolarization is then augmented by the secondary component initiated by intramuscular ICC. Each pyloric slow wave therefore reflects the sum of contributions made by myenteric plexus and intramuscular ICC (**Hirst and Edwards,2004**). In the present work, ICC in human small intestine was restricted to the myenteric plexus and the deep muscular plexus in all levels of the small intestine. However, the mean area percent of myenteric plexus ICC was always significantly higher than that of deep muscular plexus ICC. The peak value for myenteric plexus ICC was observed in duodenum while that of deep muscular plexus was noticed in jejunum. This is in agreement with the previous studies which reported ICC distribution in guinea pig (**Burns et al.,1997**), in rat (**Horiguchi and Komuro, 1998**), in mouse (**Vanderwinden et al.,2000**) and in human (**Min and Sook Soe, 2003**) small intestine using c-kit immunohistochemistry. **Nakagawa et al.(2005)** suggested that myenteric plexus ICC were essential for the generation of spontaneous intestinal peristaltic movements and they might determine the polarity of excitation so that muscle contractions could propagate from the proximal to the distal end of the small intestine. Evidence for gap junctions within the deep muscular plexus ICC network and between deep muscular plexus ICC and smooth muscle cells was reported (**Horiguchi and Komuro,1998 and Seki and Komuro, 2001**). Direct evidence for functional coupling within deep muscular plexus ICC network and between this

network and smooth muscle cells was reported by **Kobilo et al.(2003)**. All these previous studies suggested that deep muscular plexus ICC could be essential for neurotransmission in the circular muscle of small intestine.

As for the large intestine, ICC were detected at three sites; submucosal border of the circular muscle, intramuscular, and at the myenteric plexus. These results were in accordance with the previous immunohistochemical studies on ICC distribution in guinea pig colon (**Burns et al.,1997**), human colon & rectum (**Hagger et al.,1998**), human and mouse colon (**Vanderwinden et al.,2000**) and human rectum (**Shafik et al.,2004**). Segmental variations in the area percent of ICC at various levels of the muscularis externa were apparent. ICC distribution rose from a relatively low level in the cecum and appendix to a maximum in the transverse colon, declining towards the rectum. The regional variations of ICC distribution in human large intestine reported in this study were consistent with those reported by **Burns et al. (1997)** and **Hagger et al.(1998)** but contradicted with **Vanderwinden et al. (2000)**, who did not report any segmental differences. In each segment of the human large intestine, the greatest proportion of ICC was observed in the intermuscular plane in which ICC encased myenteric plexus except in the rectum and appendix, where there was no statistical significant difference between myenteric plexus and intramuscular ICC. Submucosal ICC showed the least area percent in all levels of large intestine. In human colon, regional variations in slow waves activity have been reported, and in vivo studies have demonstrated that the dominant frequency of contractions was highest in the mid-colonic region (**Sarna et al.,1980**). This finding strongly correlates with the observation that myenteric plexus ICC was greatest in the transverse colon reported in the present study. In human colon and rectum, contractile activity was characterized by propagated and non-propagated contractions. The non-propagated motor activity might reflect pacing of smooth muscle by myenteric plexus ICC. Propagated motor activity in the form of colonic motor complexes, rectal

motor complexes, or high amplitude propagated contractions would require communication through intramuscular ICC. Similarly, transmural differences in ICC might explain the initiation of segmental contractions in the colon and lack of segmental activity in the rectum which had a relatively even distribution of myenteric plexus and intramuscular ICC (**Hagger *et al.*,1998**). In the present study, many ICC were demonstrated inbetween smooth muscle fibers of the internal anal sphincter but no ICC were detected at the external anal sphincter. This is in agreement with **Piotrowska *et al.*(2003)** who reported the presence of many c-kit positive ICC among the muscle fibers in the normal internal anal sphincter. They also documented the complete absent or marked reduction of ICC in internal anal sphincter achalasia and Hirschsprung's disease which might contribute to motility dysfunction in these patients. The internal anal sphincter provides most of the resting anal pressure and is reinforced during voluntary squeeze by external anal sphincter, anal mucosal folds and anal endovascular cushions (**Rao, 2004**). **De Lorijn *et al.*(2005)** suggested that the rectoanal inhibitory reflex was mediated by nitric oxide and required an intact network of ICC in internal anal sphincter. Thus loss of nitrogenic innervation and deficiency of ICC would lead to impaired anal relaxation and may play an important role in rectal evacuation disorders. The present work could document that c-kit immunohistochemistry is a handy, reproducible and relatively reliable method to study ICC under the light microscopy in the normal human alimentary tract. The present work also indicated the presence of two morphological types of ICC which could have its reflection on the functional subclassification of these cells. ICC appeared to be sophisticated both in morphology and function. This deserves their targeting by additional research works utilizing advanced research methodologies to demonstrate any possible changes in morphology and topographical distribution in relation to sex and with advancement of age. This could allow for better characterization of the demonstrated morphological subtypes and the possible

functional differences between them. Research works should concentrate on gene regulation of these cells in a trial to restore functions of these cells in related diseases.

## REFERENCES

- 1- **Arber DA , Tamayo R and Weiss LM (1998):** Paraffin section detection of the C-kit gene product (CD117) in human tissues: value in the diagnosis of mast cell disorders. *Hum. Path.*,28:498-504.
- 2- **Bancroft JD, Cook HC(1994):** Immunohistochemistry ;In *Manual of Histological Techniques and their Diagnostic Applications* .Churchill Livingstone ,Edinburgh ,London ,Madrid ,Melbourne ,New York and Tokyo,263-293.
- 3- **Burn AJ , Lomax AE , Torihashi S, Sanders KM and Ward SM(1996):** Interstitial cells of Cajal mediate inhibitory neurotransmission in the stomach. *Proc. Nat. Acad. Sci. USA*, (Abstract) 93:12008-12013.
- 4- **Burns AJ, Herbert TM, Ward SM and Sanders KM (1997):** Interstitial cells of Cajal in the guinea-pig gastrointestinal tract as revealed by c-kit immunohistochemistry. *Cell Tissue Res.*;290:11-20.
- 5- **Christensen J, Rick G and Lowe L (1992):** Distributions of interstitial cells of Cajal in stomach and colon of cat, dog, ferret, opossum, rat, guinea pig and rabbit. *J. Auton. Nerv. Syst.*,37:47-55.
- 6- **Daniel EE and Posey-Daniel V (1984):** Neuromuscular structures in opossum esophagus: role of interstitial cells of Cajal. *Am. J. Physiol.*, 246:305-315.
- 7- **De Lorijn F, De Jonge WJ , Wedel T and Vanderwinden JM (2005):** Interstitial cells of Cajal are involved in the afferent limb of the rectoanal inhibitory reflex. *Gut*, 54(8):1107-1113.
- 8- **Farraway L, Ball AK and Huizinga JD (1995):** Intercellular metabolic coupling in canine colon musculature. *Am. J. Physiol.*, 268:1492-1502.
- 9- **Faussone-Pellegrini MS , Pantalone D and Cortesini, C (1990):** Smooth muscle cells, interstitial cells of Cajal and myenteric plexus interrelationships in the human colon. *Acta. Anat.*,139:31-44.
- 10- **Hagger R , Gharaie S , Finlayson C and Kumar D (1998):** Regional and transmural density of interstitial cells of Cajal in human colon and rectum. *Am. J. Physiol.*,38:1309-1320.
- 11- **Hanani M , Belzer V , Rich A and Faussone-Pellegrini, SM (1999):** Visualization of interstitial cells of Cajal in living, intact tissues. *Microsc. Res. Tech.*,47(5):336-343
- 12- **Hirst GD and Edwards FR (2004):** Role of interstitial cells of Cajal in the control of gastric motility. *J. Pharmacol. Sci.* ,(96):1-10.

- 13- **Horiguchi K and Komuro T (1998):** Ultrastructural characterization of interstitial cells of Cajal in the rat small intestine using control and Ws/Ws mutant rats. *Cell Tissue Res.*,293(2):277-284.
- 14- **Huizinga JD , Berezin I , Chorneyko K and Riddell RH (1998):** Interstitial cells of Cajal: pacemaker cells? *Am. J. Pathol.*,153:2001-2008 .
- 15- **Jain D, Moussa K , Tandon M , Culpepper-Morgan J and Proctor DD (2003):** Role of interstitial cells of Cajal in motility disorders of the bowel. *Am. J. Gastroenterol.*,98(3):618-624.
- 16- **Kindblom LG , Remotti HE, Aldenborg F and Meis-Kindblom JM (1998):** Gastrointestinal stomal tumors show phenotypic characteristics of the interstitial cells of Cajal. *Am. J. Pathol.*,152:1259-1269.
- 17- **Kobilo T,Szurszewski JH , Farrugia G and Hanani M (2003):** Coupling and innervation patterns of interstitial cells of Cajal in the deep muscular plexus of the guinea-pig. *Neurogastroenterol. Motil.*, 15(6):635-641.
- 18- **Komori K and Suzuki H (1986):** Distribution and properties of excitatory and inhibitory junction potentials in circular muscle of the guinea-pig stomach. *J. Physiol.*, 370:339-355.
- 19- **Langer JC , Berezin I and Daniel EE (1995):** Hypertrophic pyloric stenosis : ultrastructural abnormalities of enteric nerves and the interstitial cells of Cajal . *J. Pediatr. Surg.*,30(11):1535-1543.
- 20- **Maeda H , Yamagata A , Nishikawa S, Yoshinaga K ; Kobayashi S and Nishi K (1992):** Requirement of C-kit for development of intestinal pacemaker system. *Development*, 116:369-375.
- 21- **Manneschi IL , Pacini S, Corsani L and Bechi P(2004):** Interstitial cells of Cajal in the human stomach: distribution and relationship with enteric innervation. *Histol. Histopathol.*,19(4):1153-1164 .
- 22- **Mazet B and Raynier C (2004):** Interstitial cells of Cajal in the guinea pig gastric antrum: distribution and regional density. *Cell Tissue Res.*, 52:243-247.
- 23- **Min KW and Sook Soe I (2003):** Interstitial cells of Cajal in the human small intestine: immunochemical and ultrastructural study. *Ultrastruct. Pathol.*, 27(2):67-78.
- 24- **Mould RF(1989):**Introductory Medical Statistics,2<sup>nd</sup> ed.,Adam Hilger,Bristol ,Philadelphia, 17:126-138.
- 25- **Nakagawa T, Misawa H , Nakajima Y and Takaki M (2005):** Absence of peristalsis in the ileum of W/W(V) mutant mice that are selectively deficient in myenteric interstitial cells of Cajal. *J. Smooth Muscle Res.*,41(3):141-151.
- 26- **Nishitani A , Hirota S , Nishida T , Isozaki K and Hashimoto K (2005):** Differential expression of connexin 43 in gastrointestinal stromal tumors of gastric and small intestinal origin.*J. Pathol.*,4:222-225.
- 27- **Ortiz-Hidalgo C , De Leon Bojorge B and Albores-Saavedra J(2000):** Stromal tumor of the gall bladder with phenotype of interstitial cells of Cajal: a previously unrecognized neoplasm. *Am. J. Surg. Pathol.*,24(10):1420-1423.
- 28- **Piotrowska AP , Solari V and Puri P (2003):** Distribution of interstitial cells of Cajal in the internal anal sphincter of patients with internal anal sphincter achalasia and Hirschsprung's disease. *Arch. Pathol. Lab. Med.*,127(9):1192-1195.
- 29- **Poole DP , Hunne B , Robbins HI and Furness JB (2003):** Protein kinase C isoforms in the enteric nervous system. *Histochem. Cell Biol.*,2:155-163.
- 30- **Rao SS (2004):** Pathophysiology of adult fecal incontinence. *Gastroenterol.*, 126:14-22.
- 31- **Rumessen JJ and Thuneberg L (1996):** Pacemaker cells in the gastrointestinal tract: Interstitial cells of Cajal. *Scand. J. Gastroenterol.*,216:82-94.
- 32- **Rumessen JJ , Kerchova A , Mignon S , Bernex F and Timmermans JP (2001):** Interstitial cells of Cajal in the striated musculature of the mouse esophagus. *Cell Tissue Res.*,306(1)1-14.
- 33- **Sarna S , Bardakjian B , Waterfall W and Lind J(1980):** Human colonic electrical control activity (CEA). *Gastroenterol.*, 78:1526-1535.
- 34- **Seki K and Komuro T (2001):** Immunocytochemical demonstration of the gap junction proteins connexin 43 and connexin 45 in the musculature of the rat small intestine. *Cell Tissue Res.*,306(3):417-422.
- 35- **Shafik A , El-Sibai O , Ahmed I and Shafik AA (2004):** Identification of interstitial cells of Cajal in the human rectum. *Front. Biosci.*,9:2848-2851.
- 36- **Thuneberg L (1982):** Interstitial cells of Cajal: intestinal pacemaker cells? *Adv. Anat. Embryol. Cell. Biol.*, 71:1-30.
- 37- **Vanderwinden JM , Rumessen JJ and Liu H (1996):** Interstitial cells of Cajal in human colon and in Hirschsprung's disease. *Gastroenterol.*,111:901- 910.
- 38- **Vanderwinden JM , Rumessen ML , Vanderhaeghen JJ and Schiffmann SN (2000):** CD34 immunoreactivity and interstitial cells of Cajal in the human and mouse gastrointestinal tract. *Cell Tissue Res.*,302:145-153.
- 39- **Wang XY, Sanders KM and Ward SM (2000):** Relationship between interstitial cells of Cajal and enteric motor neurons in the murine proximal colon. *Cell Tissue Res.*,302(3):331-342 .
- 40- **Ward SM , Morris G , Reese L , Wang XY and Sanders KM (1998):** Interstitial cells of Cajal mediate enteric inhibitory neurotransmission in the lower esophageal and pyloric sphincter. *Gastroenterol.*, 115:314-329.
- 41- **Ward SM , Gershon MD , Keef K , Bayguinov YR , Nelson C and Sanders KM (2002):** Interstitial cells of Cajal and electrical activity in ganglionic and aganglionic colons of mice. *Am. J. Physiol. Gastrointest. Liver Physiol.*, 283(2):56-61.

- 42- **Wedel T, Spiegler J , Soellner S and Roblick J (2002):** Enteric nerves and interstitial cells of Cajal are altered in patients with slow-transit constipation and megacolon. *Gastroenterol.*,123:1459-1467.
- 43- **Wu M, Majewski M , Wojtkiewicz J and Vanderwinden JM(2003):** Anatomical and neurochemical features of the extrinsic and intrinsic innervation of the striated muscle in the porcine esophagus: evidence for regional and species differences. *Cell Tissue Res.*,311(3):289-297.
- 44- **Zhang Y , Zhang K , Luo J and Qi H (2002):** Changes of ultrastructure characteristics of Cajal interstitial cell in intestinal tract of diabetic rats. (English Abstract) *Zhonghua Nei Ke Za Zhi.*,41(5):310-320.

## خلايا كاجال البينية في القناة الهضمية الطبيعية الأدمية: دراسة نسيجية كيميائية مناعية

محمد عبدالحافظ، أمل مصطفى عباس، دينا رضوان، زينب المعداوى

قسم الهستولوجيا، كلية الطب، جامعة القاهرة

خلايا كاجال البينية هي خلايا متفاعلة مناعيا مع سي-كيت وتوجد في القناة الهضمية ومن المفترض أن يكون لها دور في التحكم في حركة الأمعاء. هدف هذا البحث هو دراسة شكل خلايا كاجال البينية وتقييم طريقة توزيع هذه الخلايا خلال المناطق المختلفة والطبقات المختلفة في القناة الهضمية الطبيعية للإنسان. أجريت هذه الدراسة علي 102 عينه من القناة الهضمية الطبيعية للإنسان تم الحصول عليها من مرضي ذكور متوسط أعمارهم  $37.92 \pm 8.53$ . تم الحصول علي معظم هذه العينات من الحافة الظاهرية الطبيعية لمرضي أجريت لهم جراحة لعلاج السرطان. تم التعامل مع عينات القناة الهضمية الطبيعية للإنسان وتجهيز شرائح بارافين سمكها 5 ميكرومتر. ثم صبغ جميع الشرائح من كلا المجموعتين بصبغة الهيماتوكسلين والإيوسين والصبغة الهستوكيميائية المناعية ضد سي-كيت. تم إخضاع الشرائح المصبوغة بالصبغة الهستوكيميائية المناعية إلي محلل الصورة وذلك لتحديد نسبة المساحة المتفاعلة مع الصبغة الهستوكيميائية المناعية بالنسبة للمساحة الكلية للمجال الذي تمت دراسته في شرائح القناة الهضمية الطبيعية للإنسان. ثم تم إخضاع المعلومات التي تم الحصول عليها من محلل الصورة لكل الشرائح المدروسة للتحليل الأحصائي. أوضحت الشرائح المصبوغة بصبغة الهيماتوكسلين والإيوسين التركيب الهستولوجي الطبيعي في الأجزاء المختلفة من القناة الهضمية ولكن لم يكن من الممكن إظهار خلايا كاجال البينية بصبغة الهيماتوكسلين والإيوسين الروتينية. أوضح الفحص المجهرى للشرائح المصبوغة بالصبغة الهستوكيميائية المناعية في المناطق المختلفة من القناة الهضمية الطبيعية وجود خلايا كاجال البينية المتفاعلة مناعيا والتي ظهرت كخلايا مغزلية لها تفرعات شجرية ثنائية القطبين أو متعددة الأقطاب. اختلفت طريقة توزيع خلايا كاجال البينية في المناطق المختلفة من القناة الهضمية حيث تم تحديد خلايا كاجال البينية في طبقة الضفيرة العصبية المتعلقة بعضل الأمعاء في كل من المرئ وجسم المعدة وبواب المعدة والأمعاء الدقيقة والقولون والمستقيم. كان من الممكن إظهار خلايا كاجال البينية الموجودة داخل طبقات العضلات في كل من المرئ وقعر المعدة وجسم المعدة وبواب المعدة والقولون والمستقيم والقناة الشرجية. أما خلايا كاجال الموجودة في طبقة الضفيرة العصبية العضلية العميقة فقد وجدت في الأمعاء الدقيقة فقط. في بواب المعدة والقولون والمستقيم تم العثور علي خلايا كاجال البينية في الحد الذي يفصل طبقة تحت الغشاء المخاطي عن طبقة العضلات الدائرية.